

Trends in Ground-State Entropies for Transition Metal Based Hydrogen Atom Transfer Reactions

Elizabeth A. Mader,^{†,§,*} Virginia W. Manner,[†] Todd F. Markle,[†] Adam Wu,[†] James A. Franz,[‡] and James M. Mayer^{†,*}

Department of Chemistry, University of Washington, Box 351700, Seattle, Washington 98195-1700, and Chemical & Materials Sciences Division, Pacific Northwest National Laboratory, P.O. Box 999, Richland, Washington 99352

Received October 17, 2008; E-mail: mayer@chem.washington.edu

Abstract: Reported herein are thermochemical studies of hydrogen atom transfer (HAT) reactions involving transition metal H-atom donors M^{II}LH and oxyl radicals. [Fe^{II}(H₂bip)₃]²⁺, [Fe^{II}(H₂bim)₃]²⁺, [Co^{II}(H₂bim)₃]²⁺, and Ru^{II}(acac)₂(py-imH) [H₂bip = 2,2'-bi-1,4,5,6-tetrahydropyrimidine, H₂bim = 2,2'-bi-imidazoline, acac = 2,4-pentandionato, py-imH = 2-(2'-pyridyl)imidazole] each react with TEMPO (2,2,6,6-tetramethyl-1-piperidinoxyl) or ^tBu₃PhO[•] (2,4,6-tri-*tert*-butylphenoxyl) to give the deprotonated, oxidized metal complex M^{III}L and TEMPOH or ^tBu₃PhOH. Solution equilibrium measurements for the reaction of [Co^{II}(H₂bim)₃]²⁺ with TEMPO show a large, negative ground-state entropy for hydrogen atom transfer, $-41 \pm 2 \text{ cal mol}^{-1} \text{ K}^{-1}$. This is even more negative than the $\Delta S^{\circ}_{\text{HAT}} = -30 \pm 2 \text{ cal mol}^{-1} \text{ K}^{-1}$ for the two iron complexes and the $\Delta S^{\circ}_{\text{HAT}}$ for Ru^{II}(acac)₂(py-imH) + TEMPO, $4.9 \pm 1.1 \text{ cal mol}^{-1} \text{ K}^{-1}$, as reported earlier. Calorimetric measurements quantitatively confirm the enthalpy of reaction for [Fe^{II}(H₂bip)₃]²⁺ + TEMPO, thus also confirming $\Delta S^{\circ}_{\text{HAT}}$. Calorimetry on TEMPOH + ^tBu₃PhO[•] gives $\Delta H^{\circ}_{\text{HAT}} = -11.2 \pm 0.5 \text{ kcal mol}^{-1}$ which matches the enthalpy predicted from the difference in literature solution BDEs. A brief evaluation of the literature thermochemistry of TEMPOH and ^tBu₃PhOH supports the common assumption that $\Delta S^{\circ}_{\text{HAT}} \approx 0$ for HAT reactions of organic and small gas-phase molecules. However, this assumption does not hold for transition metal based HAT reactions. The trend in magnitude of $|\Delta S^{\circ}_{\text{HAT}}|$ for reactions with TEMPO, Ru^{II}(acac)₂(py-imH) \ll [Fe^{II}(H₂bip)₃]²⁺ = [Fe^{II}(H₂bim)₃]²⁺ $<$ [Co^{II}(H₂bim)₃]²⁺, is surprisingly well predicted by the trends for electron transfer half-reaction entropies, $\Delta S^{\circ}_{\text{ET}}$, in aprotic solvents. This is because both $\Delta S^{\circ}_{\text{ET}}$ and $\Delta S^{\circ}_{\text{HAT}}$ have substantial contributions from vibrational entropy, which varies significantly with the metal center involved. The close connection between $\Delta S^{\circ}_{\text{HAT}}$ and $\Delta S^{\circ}_{\text{ET}}$ provides an important link between these two fields and provides a starting point from which to predict which HAT systems will have important ground-state entropy effects.

1. Introduction

The transfer of a hydrogen atom, reaction 1, is one of the most fundamental chemical transformations. It is a cornerstone of organic free-radical chemistry, from combustion to the *in vitro* and *in vivo* action of antioxidants.¹ In recent years, it has



become clear that this reaction is also involved in a variety of metal-mediated oxidations, including coordination complexes, metalloenzyme active sites, and metal-oxide surfaces.^{2–5} For example, both plants and animals employ lipoxygenases to catalyze the selective hydroperoxidation of 1,4 diene units in fatty acids by using hydrogen transfer to an iron(III) hydroxide species.⁶ Reaction 1 has also been implicated in catalysis by other metalloenzymes such as cytochrome P450,⁷ methane monooxygenases,⁸ and class I ribonucleotide reductases.^{3a,9}

[†] University of Washington.

[‡] Pacific Northwest National Laboratory.

[§] Current address: Chemical Sciences and Engineering Division, Argonne National Laboratory, 9700 S. Cass Ave., Argonne, IL, 60439-4801.

(1) (a) *Free Radicals*; Kochi, J. K., Ed.; Wiley: New York, 1973, especially Ingold, K. U. Vol. 1, Chapter 1, pp 67ff; Russell, G. A. Vol. 1, Chapter 7, pp 275–331; and O'Neal, H.; Benson, S. W. Vol. 2, Chapter 17, pp 275–359. *Radical Reaction Rates in Liquids*; Landolt-Börnstein New Series; Fischer, H., Ed.; Springer-Verlag: Berlin, (b) 1984; Vol. 13, subvol. a–e; (c) 1994; Vol. 18, subvol. A–E. (d) Hendry, D. G.; Mill, T.; Piskiewicz, L.; Howard, J. A.; Eigenmann, H. K. *J. Phys. Chem. Ref. Data* **1974**, 3, 937–978. (e) Fossey, J.; Lefort, D. Sorba, J. *Free Radicals in Organic Chemistry*; Wiley: New York, 1995. (f) Leffler, J. E. *An Introduction to Free Radicals*; Wiley: New York, 1993; Chapters 7–8. (g) Halliwell, B.; Gutteridge, J. M. C. *Free Radicals in Biology and Medicine*; Oxford University Press: New York, 1999. (h) *Oxidative Stress: Oxidants and Antioxidants*; Sies, H., Ed.; Academic: New York, 1991. (i) *Active Oxygen in Chemistry*; Foote, C. S., Valentine, J. S., Liebman, J., Greenberg, A., Eds.; Blackie, Chapman and Hall: Glasgow, 1995.

(2) (a) *Hydrogen-Transfer Reactions*; Hynes, J. T., Klinman, J. P., Limback, H.-H., Schowen, R. L., Eds.; Wiley-VCH: Weinheim, 2007. (b) See also footnotes 6–14.

(3) (a) Stubbe, J.; van der Donk, W. A. *Chem. Rev.* **1998**, 98, 705–762. (b) Pesavento, R. P.; van der Donk, W. A. *Adv. Protein Chem.* **2001**, 58, 317–385. (c) Marsh, E. N. G. *BioEssays* **1995**, 17, 431–441. (d) Pierre, J. L.; Thomas, F. C. R. *Chim.* **2005**, 8, 65–74. (e) Fontecave, M.; Pierre, J. L. C. R. *Acad. Sci., Ser. IIc* **2001**, 4, 531–538. (f) Decker, A.; Chow, M. S.; Kemsley, J. N.; Lehnert, N.; Solomon, E. I. *J. Am. Chem. Soc.* **2006**, 128, 4719–4733.

(4) (a) Labinger, J. A. *J. Mol. Catal. A* **2004**, 220, 27–35. (b) Labinger, J. A. *Catal. Lett.* **1988**, 1, 371–376. (c) Limberg, C. *Angew. Chem., Int. Ed.* **2003**, 42, 5932–5954.

Cobaloximes, cobalt-porphyrins, and chromium cyclopentadienyl compounds effect chain transfer in living radical polymerizations using reaction 1.¹⁰ Developing a fundamental understanding of hydrogen transfer is thus broadly important.

Reaction 1, which we will call hydrogen atom transfer (HAT),¹¹ is part of a broad class of processes involving proton and electron transfer, often called proton-coupled electron transfer (PCET).^{12–14} Theoretical treatments of PCET, like their antecedent theories of electron transfer (ET)¹⁵ and proton transfer (PT),¹⁶ use free energies (ΔG) as measures of reaction driving force.⁵ In contrast, analyses of HAT reactions have typically used the enthalpic driving force, as in the Bell–Evans–Polanyi equation (BEP) that relates the activation barrier to the

ΔH .^{1a,17} ΔH° for an HAT reaction is the difference in bond dissociation enthalpies (BDEs) between the reactant A–H and the product B–H. In our view, the BEP correlation is a primary historical reason why chemists have focused on BDEs, rather than bond dissociation free energies (BDFEs).

The focus on enthalpies to understand HAT reactions is surprising since reactivity typically is correlated with free energies, as in linear *free energy* relationships (LFERs).¹⁸ These treatments are equivalent when the entropies of reaction are close to zero (when $\Delta S^\circ = 0$, $\Delta G^\circ = \Delta H^\circ$), as has been assumed in most treatments of hydrogen atom transfer (with a few exceptions¹⁹). The assumption that $\Delta S^\circ \approx 0$ is also part of the foundation for the increasingly common determination of BDEs from solution pK_a and $E_{1/2}$ values, as popularized by Bordwell and co-workers.^{20–25}

The assumption that ΔS° is ~ 0 appears to hold for HAT reactions of small molecules in the gas phase²⁶ and of larger organics in solution,²⁷ but HAT reactions of two iron complexes have recently been shown to have very large $|\Delta S^\circ_{\text{HAT}}|$.²⁸ For

- (5) (a) Hammes-Schiffer, S. *Acc. Chem. Res.* **2001**, *34*, 273–281. (b) Cukier, R. I. *J. Phys. Chem. B* **2002**, *106*, 1746–1757. (c) Kuznetsov, A. M.; Ulstrup, J. *Can. J. Chem.* **1999**, *77*, 1085–1096. (d) Krishtalik, L. I. *Biochim. Biophys. Acta* **2000**, *1458*, 6–27. (e) Hatcher, E.; Soudackov, A.; Hammes-Schiffer, S. *Chem. Phys.* **2005**, *319*, 93–100. (f) Cukier, R. I. *ACS Symp. Series* **2004**, *883*, 145158 (Molecular Bioenergetics).
- (6) (a) Liang, Z.-X.; Klinman, J. P. *Curr. Opin. Struct. Biol.* **2004**, *14*, 648–655. (b) Hatcher, E.; Soudackov, A. V.; Hammes-Schiffer, S. *J. Am. Chem. Soc.* **2004**, *126*, 5763–5775. (c) Lehnert, N.; Solomon, E. I. *J. Biol. Inorg. Chem.* **2003**, *8*, 294–305. (d) Goldsmith, C. R.; Stack, T. D. P. *Inorg. Chem.* **2006**, *45*, 6048–6055. (e) Costas, M.; Mehn, M. P.; Jensen, M. P.; Que, L. *Chem. Rev.* **2004**, *104*, 939–986.
- (7) (a) Kaizer, J.; Klinker, E. J.; Oh, N. Y.; Rohde, J.-U.; Song, W. J.; Stubna, A.; Kim, J.; Munck, E.; Nam, W.; Que, L., Jr. *J. Am. Chem. Soc.* **2004**, *126*, 472–473. (b) de Visser, S. P.; Kumar, D.; Cohen, S.; Shacham, R.; Shaik, S. *J. Am. Chem. Soc.* **2004**, *126*, 8362–8363. (c) Kumar, D.; de Visser, S. P.; Shaik, S. *J. Am. Chem. Soc.* **2004**, *126*, 5072–5073. (d) Schlichting, I.; Berendzen, J.; Chu, K.; Stock, A. M.; Maves, S. A.; Benson, D. E.; Sweet, R. M.; Ringe, D.; Petsko, G. A.; Sliagar, S. G. *Science* **2000**, *287*, 1615–1622.
- (8) (a) Ragsdale, S. W. *Chem. Rev.* **2006**, *106*, 3317–3337. (b) Baik, M.-H.; Newcomb, M.; Friesner, R. A.; Lippard, S. J. *Chem. Rev.* **2003**, *103*, 2385–2419. (c) Brazeau, B. J.; Austin, R. N.; Tarr, C.; Groves, J. T.; Lipscomb, J. D. *J. Am. Chem. Soc.* **2001**, *123*, 11831–11837.
- (9) (a) Stubbe, J.; Nocera, D. G.; Yee, C. S.; Chang, M. C. Y. *Chem. Rev.* **2003**, *103*, 2167–2201. (b) Reece, S. Y.; Hodgkiss, J. M.; Stubbe, J.; Nocera, D. G. *Philos. Trans. R. Soc. London, Ser. B* **2006**, *361*, 1351–1364.
- (10) Gridnev, A. A.; Ittel, S. D. *Chem. Rev.* **2001**, *101*, 3611–3659.
- (11) The terminology in the PCET area is in flux. A number of papers, including some of ours, define HAT very narrowly.^{12,13b–d} A recent major review defines HAT as a reaction in which “both the transferring electron and proton come from the same bond” (ref 12a, p 5024). This mechanistic distinction is, however, often problematic to apply in practice. Therefore in cases when the intimate details are not at issue, we prefer a broad definition of HAT that encompasses all processes involving concerted movement of a proton and an electron ($e^- + H^+ \equiv H^\bullet$) in a single kinetic step, when both the proton and the electron originate from the same reactant and travel to the same product.^{13a} The metal-containing reactions 4–7 here are HAT in the broad definition but excluded under the narrower ones, because the transferred H^+ forms a N–H σ -bond while the e^- formally adds to a different orbital, a metal π -symmetry t_{2g} -type orbital. The organic reaction of $t\text{-Bu}_3\text{ArO}^\bullet + \text{TEMPOH}$ (eq 8), under the definition quoted above,^{12a} would be considered HAT in the forward direction but not in the reverse direction (assuming that the phenolic H lies in the plane of the aromatic ring).
- (12) (a) Huynh, M. H. V.; Meyer, T. J. *Chem. Rev.* **2007**, *107*, 5004–5064. (b) Cukier, R. I.; Nocera, D. G. *Annu. Rev. Phys. Chem.* **1998**, *49*, 337–369. (c) Stubbe, J.; Nocera, D. G.; Yee, C. S.; Chang, M. C. Y. *Chem. Rev.* **2003**, *103*, 2167–2202. (d) Meyer, T. J.; Huynh, M. H. V. *Inorg. Chem.* **2003**, *42*, 8140–8160. (e) Lebeau, E. L.; Binstead, R. A.; Meyer, T. J. *J. Am. Chem. Soc.* **2001**, *123*, 10535–10544. (f) Chen, X.; Bu, Y. *J. Am. Chem. Soc.* **2007**, *129*, 9713–9720. (g) Cowlet, R. E.; Bontchev, R. P.; Sorrell, J.; Sarrachino, O.; Feng, Y.; Wang, H.; Smith, J. M. *J. Am. Chem. Soc.* **2007**, *129*, 2424–2425.
- (13) (a) Mayer, J. M. *Annu. Rev. Phys. Chem.* **2004**, *55*, 363–390. (b) Mayer, J. M.; Hrovat, D. A.; Thomas, J. L.; Borden, W. T. *J. Am. Chem. Soc.* **2002**, *124*, 11142–11147. (c) Litwinenko, G.; Ingold, K. U. *Acc. Chem. Res.* **2007**, *40*, 222–230. (d) Tishchenko, O.; Truhlar, D. G.; Ceulemans, A.; Nguyen, M. T. *J. Am. Chem. Soc.* **2008**, *130*, 7000–7010.
- (14) (a) Ref 12a. (b) Manner, V. W.; DiPasquale, A. G.; Mayer, J. M. *J. Am. Chem. Soc.* **2008**, *130*, 7210–7211. (c) Warren, J. J.; Mayer, J. M. *J. Am. Chem. Soc.* **2008**, *130*, 2774–2776. (d) Mayer, J. M.; Rhile, I. J. *Biochim. Biophys. Acta* **2004**, *1655*, 51–58. (e) Mayer, J. M.; Rhile, I. J.; Larsen, F. B.; Mader, E. A.; Markle, T. F.; DiPasquale, A. G. *Photosynth. Res.* **2006**, *87* (1), 3–20, and 21–24. (f) Mayer, J. M.; Mader, E. A.; Roth, J. P.; Bryant, J. R.; Matsuo, T.; Dehestani, A.; Bales, B. C.; Watson, E. J.; Osako, T.; Valliant-Saunders, K.; Lam, W.-H.; Hrovat, D. A.; Borden, W. T.; Davidson, E. R. *J. Mol. Catal. A* **2006**, *251*, 24–33.
- (15) (a) Marcus, R. A.; Sutin, N. *Biochim. Biophys. Acta* **1985**, *811*, 265–322. (b) Marcus, R. A.; Sutin, N. *Inorg. Chem.* **1975**, *14*, 213–216.
- (16) Kiefer, P. M.; Hynes, J. T. *J. Phys. Chem. A* **2004**, *108*, 11809–11818, and references therein.
- (17) (a) Shaik, S. S.; Schlegel, H. B.; Wolfe, S. *Theoretical Aspects of Physical Organic Chemistry: The S_N2 Reaction*; John Wiley & Sons, Inc.: New York, 1992. (b) Knox, J. H. Rate constants in the gas-phase oxidation of alkanes and alkyl radicals. In *Advances in Chemistry Series*; American Chemical Society: 1968; Vol. 76, pp 1–22. (c) Cohen, N.; Benson, S. W. *J. Phys. Chem.* **1987**, *91*, 171–175. (d) Senkan, S. M.; Quam, D. J. *J. Phys. Chem.* **1992**, *96*, 10837–10842. (e) Tsang, W. In *Energetics of Organic Free Radicals*; Simões, J. A. M., Greenberg, A., Liebman, J. F., Eds.; Blackie, NY, 1996; Chapter 2, pp 22–58.
- (18) (a) Lowry, T. H.; Richardson, K. E. *Mechanism and Theory in Organic Chemistry*; Harper & Row Publishers: San Francisco, 1976. (b) Smith, M. B.; March, J. *March's Advanced Organic Chemistry*, 5th ed.; Wiley-Interscience: New York, 2001.
- (19) The temperature dependence of ΔG_{PCET} is discussed in: (a) Pu, J.; Gao, J.; Truhlar, D. G. *Chem. Rev.* **2006**, *106*, 3140–3169. (b) Gao, J.; Ma, S.; Major, D. T.; Nam, K.; Pu, J.; Truhlar, D. G. *Chem. Rev.* **2006**, *106*, 3188–3209. (c) Costentin, C.; Robert, M.; Savéant, J.-M. *J. Am. Chem. Soc.* **2007**, *129*, 9953–9963. (d) Costentin, C.; Robert, M.; Savéant, J.-M. *J. Am. Chem. Soc.* **2006**, *128*, 4552–4553. (e) Markle, T. F.; Rhile, I. J.; DiPasquale, A. G.; Mayer, J. M. *Proc. Natl. Acad. Sci. U.S.A.* **2008**, *105*, 8185–8190. (f) Rhile, I. J.; Markle, T. F.; Nagao, K.; DiPasquale, A. G.; Lam, O. P.; Lockwood, M. A.; Rotter, K.; Mayer, J. M. *J. Am. Chem. Soc.* **2006**, *128*, 6075–6088. (g) Costentin, C. *Chem. Rev.* **2008**, *108*, 2145–2179.
- (20) Tilsted, M. The thermodynamics of organometallic systems involving electron transfer paths. In *Electron Transfer in Chemistry*; Balzani, V., Ed.; Wiley-VCH: Weinheim, 2001; Vol. 2, pp 677–713.
- (21) (a) Wiberg, K. B.; Foster, G. *J. Am. Chem. Soc.* **1961**, *83*, 423–429 (thermochemical cycle is on p 425). (b) Ebersson, L. *Acta Chem. Scand.* **1963**, *17*, 2004–2018. (c) Juan, B.; Scharz, J.; Breslow, R. *J. Am. Chem. Soc.* **1980**, *102*, 5741–5748, and references therein.
- (22) Leading references: (a) Bordwell, F. G.; Cheng, J.-P.; Ji, G.-Z.; Satish, A. V.; Zhang, X. *J. Am. Chem. Soc.* **1991**, *113*, 9790–9795. (b) Bordwell, F. G.; Cheng, J.-P.; Harrelson, J. A., Jr. *J. Am. Chem. Soc.* **1988**, *110*, 1229–1231. (c) Bordwell, F. G.; Satish, A. V.; Zhang, S.; Zhang, X.-A. *Pure Appl. Chem.* **1995**, *67* (5), 735–740. (d) Cheng, J. P.; Liu, B.; Zhao, Y. Y.; Wen, Z.; Sun, Y. K. *J. Am. Chem. Soc.* **2000**, *122*, 9987–9992.
- (23) Bordwell, F. G.; Liu, W.-Z. *J. Am. Chem. Soc.* **1996**, *118*, 10819–10823.

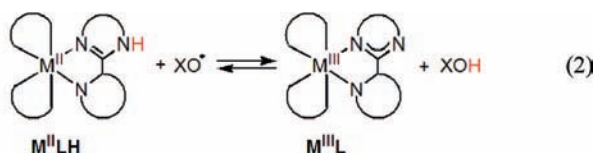
Table 1. Equilibrium Constants and Ground State Thermodynamics for Hydrogen Atom Transfer Reactions in MeCN

AH + B	method ^a	K_{eq} (298 K)	$\Delta G_{\text{HAT}}^{\circ}$ (kcal mol ⁻¹)	$\Delta H_{\text{HAT}}^{\circ}$ (kcal mol ⁻¹)	$\Delta S_{\text{HAT}}^{\circ}$ (cal mol ⁻¹ K ⁻¹)
Fe^{II}(H₂bip) + TEMPO	VH ^b	1.7 ± 0.3	-0.3 ± 0.2	-9.4 ± 0.6	-30 ± 2
	Cal	--	--	-8.9 ± 0.6	--
	BDFE	~2	-0.5 ± 1	--	--
Fe^{II}(H₂bim) + TEMPO	VH ^b	(2.0 ± 0.3) × 10 ⁻⁴	5.0 ± 0.2	-4.1 ± 0.3	-30 ± 2
	BDFE	~0.9 × 10 ⁻⁴	5.5 ± 1.0	--	--
Ru^{II}(py-imH) + TEMPO	VH ^c	(1.8 ± 0.2) × 10 ³	-4.4 ± 0.1	-3.0 ± 0.3	4.9 ± 1.1
	BDFE	(2.0 ± 1.5) × 10 ³	-4.5 ± 0.4	--	--
Co^{II}(H₂bim) + TEMPO	VH	(5.9 ± 0.8) × 10 ⁻³	3.0 ± 0.4	-9.3 ± 0.4	-41 ± 2
	BDFE	~0.6	0.3 ± 3 ^d	--	--
Ru^{II}(py-imH) + ^tBu₃PhO[•]	BDE	--	--	-15 ± 1	--
Ru^{II}(hfac)₂(py-imH) + ^tBu₃PhO[•]	VH	0.062 ± 0.013	1.6 ± 0.1	--	--
Co^{II}(H₂bim) + ^tBu₃PhO[•]	BDE	--	--	-24 ± 4	--
TEMPOH + ^tBu₃PhO[•]	Cal	--	--	-11.2 ± 0.5	--
	BD(F)E	--	-10 ± 1	-11.5 ± 1.4	-2 ± 3

^a Method: VH (van't Hoff) = Temperature dependence of K_{eq} from van't Hoff plots; Cal = calorimetric; BDFE/BDE; $\Delta G_{\text{HAT}}^{\circ} = \text{BDFE}[\text{AH}] - \text{BDFE}[\text{BH}]$ and/or $\Delta H_{\text{HAT}}^{\circ} = \text{BDE}[\text{AH}] - \text{BDE}[\text{BH}]$, using values from Table 2. ^b Data from ref 28. ^c Data from ref 32. ^d Estimated from BDFEs derived from $\text{p}K_{\text{a}}$ and E° values; see Table 2

instance, H-atom transfer from $[\text{Fe}^{\text{II}}(\text{H}_2\text{bip})_3]^{2+}$ to TEMPO ($\text{H}_2\text{bip} = 2,2'$ -bi-1,4,5,6-tetrahydropyrimidine) has $\Delta S_{\text{HAT}}^{\circ} = -30 \pm 2 \text{ cal mol}^{-1} \text{ K}^{-1}$.²⁸ In this case, $T\Delta S_{\text{HAT}}^{\circ} = -8.9 \text{ kcal mol}^{-1}$ at 298 K, a change in K_{eq} of 4×10^6 . This large $|\Delta S_{\text{HAT}}^{\circ}|$ originates primarily from a change in vibrational entropy upon a redox change at the iron center,²⁸ which suggests that HAT reactions of other metal systems may also have large values of $|\Delta S^{\circ}|$.

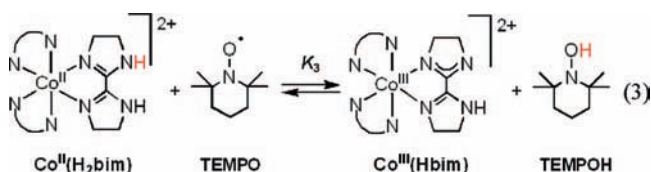
Herein, we report calorimetric and equilibrium measurements of ground-state enthalpies and entropies for a series of HAT reactions.²⁹ These reactions involve iron, cobalt, and ruthenium complexes with unsaturated nitrogen ligands, of the general type shown in eq 2. These thermodynamic measurements are used to elucidate trends in the magnitude of ground-state entropies for hydrogen atom transfer reactions, $\Delta S_{\text{HAT}}^{\circ}$.



2. Results

2.1. Equilibrium Studies. 2.1.1. Co^{II}(H₂bim) + TEMPO.

$[\text{Co}^{\text{II}}(\text{H}_2\text{bim})_3]^{2+}$ [**Co^{II}(H₂bim)**]; $\text{H}_2\text{bim} = 2,2'$ -bi-2-imidazoline; 10 mM) reacts with the stable nitroxyl radical TEMPO (3–15 equiv) in CD_3CN to give an equilibrium mixture with $[\text{Co}^{\text{III}}(\text{Hbim})(\text{H}_2\text{bim})_2]^{2+}$ [**Co^{III}(Hbim)**] and TEMPOH (eq 3; $\text{N}=\text{N} = \text{H}_2\text{bim}$). Equilibrium is reached within approximately 48 h at 298 K under these conditions.



In the reverse direction, **Co^{III}(Hbim)** plus excess TEMPOH gives complete formation of **Co^{II}(H₂bim)** and TEMPO over the course of 4 h. This reaction has been very briefly described in a previous report.³⁰ The equilibrium constant K_3 has been determined by integrating ¹H NMR spectra of reaction mixtures. All four species have easily observable ¹H NMR spectra over the temperature range studied, even though **Co^{II}(H₂bim)** and TEMPO are both paramagnetic. The average for three experi-

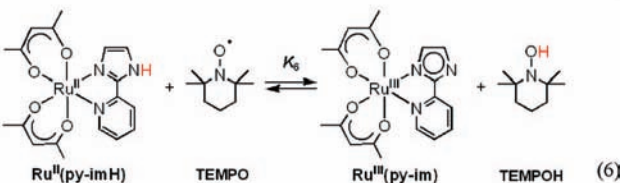
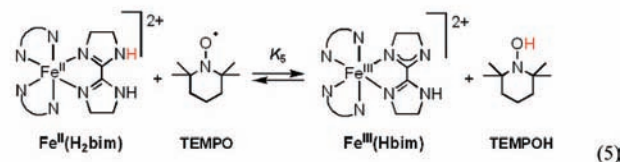
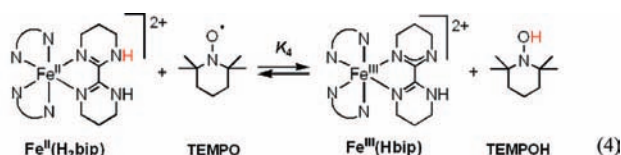
ments gives $K_3 = (5.9 \pm 0.8) \times 10^{-3}$ at 298 K, $\Delta G_{\text{HAT}}^{\circ} = 3.0 \pm 0.4 \text{ kcal mol}^{-1}$ (Table 1). This value for $\Delta G_{\text{HAT}}^{\circ}$ is within the error of the previous estimate ($+0.3 \pm 3 \text{ kcal mol}^{-1}$) derived from the relevant $\text{p}K_{\text{a}}$ and E° values.³⁰ The large error in the previous estimate is due to the poor electrochemical response of **Co^{III}(H₂bim)**.³¹

K_3 was measured from 274–313 K and found to vary by an order of magnitude over this 40 °C range (Figure 1A). van't Hoff analysis yields $\Delta H_{\text{HAT}}^{\circ} = -9.3 \pm 0.4 \text{ kcal mol}^{-1}$ and $\Delta S_{\text{HAT}}^{\circ} = -41 \pm 2 \text{ cal mol}^{-1} \text{ K}^{-1}$ (Table 1). For each sample, after measurements were complete at the high and low temperatures, the NMR tubes were allowed to re-equilibrate at room temperature (294 K). In each case, the ratio of species readjusted to values consistent with the predicted K_3 at 294 K (Figure 1A), indicating that this is a true equilibrium. Over a week at these

- (24) A subset of the references using BDE's are: (a) Parker, V. D.; Handoo, K. L.; Roness, F.; Tilset, M. *J. Am. Chem. Soc.* **1991**, *113*, 7493–7498. (b) Tilset, M.; Parker, V. D. *J. Am. Chem. Soc.* **1990**, *112*, 2843–2843. (c) Tilset, M.; Parker, V. D. *J. Am. Chem. Soc.* **1989**, *111*, 6711–6717. (d) Borovik, A. S. *Acc. Chem. Res.* **2005**, *38*, 54–61. (e) Zhang, J.; Grills, D. C.; Huang, K. W.; Fujita, E.; Bullock, R. M. *J. Am. Chem. Soc.* **2005**, *127*, 15684–15685. (f) Carrell, T. G.; Bourles, E.; Lin, M.; Dismukes, G. C. *Inorg. Chem.* **2003**, *42*, 2849–2858. (g) Astruc, D. *Acc. Chem. Res.* **2000**, *33*, 287–298. (h) Wang, D.; Angelici, R. J. *J. Am. Chem. Soc.* **1996**, *118*, 935–942. (i) Eisenberg, D. C.; Norton, J. R. *Isr. J. Chem.* **1991**, *31*, 55–66. (j) Simões, J. A. M.; Beauchamp, J. L. *Chem. Rev.* **1990**, *90*, 629–688.
- (25) For a few studies using bond dissociation free energies (BDFEs), see: (a) Fu, X.; Wayland, B. B. *J. Am. Chem. Soc.* **2005**, *127*, 16460–16467, and references therein. (b) Miedaner, A.; Raebinger, J. W.; Curtis, C. J.; Miller, S. M.; DuBois, D. L. *Organometallics* **2004**, *23*, 2670–2679. (c) Ellis, W. W.; Miedaner, A.; Curtis, C. J.; Gibson, D. H.; DuBois, D. L. *J. Am. Chem. Soc.* **2002**, *124*, 1926–1932.
- (26) Blanksby, S. J.; Ellison, G. B. *Acc. Chem. Res.* **2003**, *36*, 255–263.
- (27) (a) Lucarini, M.; Pedulli, G. F.; Cipollone, M. *J. Org. Chem.* **1994**, *59*, 5063–5070. (b) Lucarini, M.; Pedrielli, P.; Pedulli, G. F.; Valgimigli, L.; Gignes, D.; Tordo, P. *J. Am. Chem. Soc.* **1999**, *121*, 11546–11553.
- (28) Mader, E. A.; Davidson, E. R.; Mayer, J. M. *J. Am. Chem. Soc.* **2007**, *129*, 5153–5166.
- (29) The reactions examined here are net hydrogen atom transfers. Other work in progress in our laboratories indicates that they follow a concerted HAT mechanism as well, but this is independent of the thermochemical results here. See refs 28, 31.
- (30) Roth, J. P.; Yoder, J. C.; Won, T. J.; Mayer, J. M. *Science* **2001**, *294*, 2524–2526.
- (31) Yoder, J. C.; Roth, J. P.; Gussenhoven, E. M.; Larsen, A. S.; Mayer, J. M. *J. Am. Chem. Soc.* **2003**, *125*, 2629–2640.
- (32) (a) Wu, A.; Masland, J.; Swartz, R. D.; Kaminsky, W.; Mayer, J. M. *Inorg. Chem.* **2007**, *46*, 11190–11201. (b) Wu, A.; Mayer, J. M. *J. Am. Chem. Soc.* **2008**, *130*, 14745–14754.

concentrations, there is no observable decrease in the cobalt mass balance relative to the NMR integration standard, though there is slight decomposition (ca. 5%) of the excess TEMPOH.

2.1.2. $[\text{Fe}^{\text{II}}(\text{H}_2\text{bip})_3]^{2+}$, $[\text{Fe}^{\text{II}}(\text{H}_2\text{bim})_3]^{2+}$, and $\text{Ru}^{\text{II}}(\text{acac})_2(\text{py-imH}) + \text{TEMPO}$. Equilibrium constants have been reported for the reactions of TEMPO with $[\text{Fe}^{\text{II}}(\text{H}_2\text{bip})_3]^{2+}$ [$\text{Fe}^{\text{II}}(\text{H}_2\text{bip})$], $[\text{Fe}^{\text{II}}(\text{H}_2\text{bim})_3]^{2+}$ [$\text{Fe}^{\text{II}}(\text{H}_2\text{bim})$], and $\text{Ru}^{\text{II}}(\text{acac})_2(\text{py-imH})$ [$\text{Ru}^{\text{II}}(\text{py-imH})$] (eqs 4–6; H_2bip = 2,2'-bi-1,4,5,6-tetrahydro-pyrimidine; acac = 2,4-pentanedionato, py-imH = 2-(2'-pyridyl)-imidazole).^{28,32} In the iron systems, K_4 and K_5 in MeCN were determined both by static methods (as above) and from the ratio of the opposing second-order rate constants; the ruthenium K_6 was measured by UV–vis spectroscopic titration. The temperature dependence of these equilibrium constants yield the ΔH° and ΔS° values given in Table 1. K_6 is much less temperature dependent than either the iron or cobalt systems discussed above, varying by barely a factor of 1.5 over the 41 °C temperature range examined 269–310 K (Figure 1B). For the ruthenium hexafluoro-acac derivative $[\text{Ru}^{\text{II}}(\text{hfac})_2(\text{py-imH})]$, HAT to the stable and isolable³³ free radical ${}^t\text{Bu}_3\text{PhO}^\bullet$ (eq 7): $K_7 = 0.062 \pm 0.013$ at 298 K (hfac = 1,1,1,5,5,5-hexafluoro-2,4-pentanedionato, $\text{CF}_3\text{C}(\text{O})\text{CHC}(\text{O})\text{CF}_3$).³²



2.2. Calorimetry. Solution calorimetry experiments have been done to independently confirm the ground-state enthalpy values determined from the van't Hoff analyses above. A Setaram C-80 Calvet calorimeter was outfitted with a pair of Hastelloy dual chamber reversal cells and run under isothermal conditions. In a typical experiment, separate solutions of $\text{Fe}^{\text{II}}(\text{H}_2\text{bip})$ and TEMPO were thermally equilibrated under nitrogen in separate chambers of one cell. Excess TEMPO (8–34 equiv) was used to ensure that the reaction went to completion. The second cell contained an identical volume of MeCN and acted as a reference.

- (33) Manner, V. W.; Markle, T. F.; Freudenthal, J.; Roth, J. P.; Mayer, J. M. *Chem. Commun.* **2008**, 2, 256–258.
 (34) Mahoney, L. R.; Ferris, F. C.; Ingold, K. U. *J. Am. Chem. Soc.* **1969**, *91*, 3883–3889.
 (35) Mahoney, L. R.; Mendenhall, G. D.; Ingold, K. U. *J. Am. Chem. Soc.* **1973**, *95*, 8610–8614.
 (36) Roth, J. P.; Lovell, S.; Mayer, J. M. *J. Am. Chem. Soc.* **2000**, *122*, 5486–5498.
 (37) Benson, S. W. *Thermochemical Kinetics*, 2nd Edition; Wiley: New York, 1976.

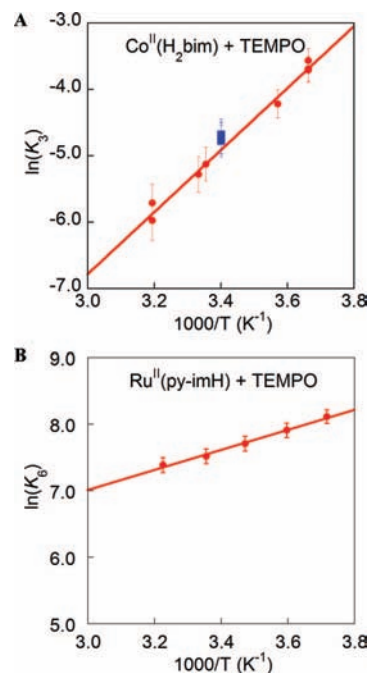


Figure 1. van't Hoff plots (A) for $\text{Co}^{\text{II}}(\text{H}_2\text{bim}) + \text{TEMPO}$ (eq 3) (●), with (■) indicating reactions that were initially run at high and low temperatures and then re-equilibrated back to 294 K, and (B) for the much less temperature dependent $\text{Ru}^{\text{II}}(\text{py-imH}) + \text{TEMPO} \rightleftharpoons \text{Ru}^{\text{III}}(\text{py-im}) + \text{TEMPOH}$ (eq 6). Plot B adapted, with permission, from ref 32b.

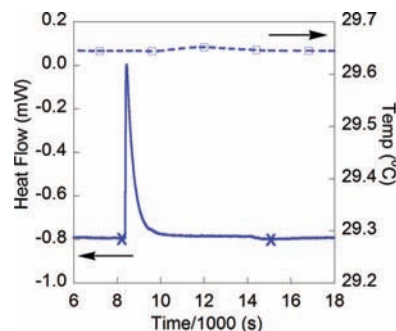


Figure 2. Heat flow curve (—) and sample temperature (---) for the reaction between 3.2 mM $\text{Fe}^{\text{II}}(\text{H}_2\text{bip})$ and 0.10 M TEMPO in MeCN. The “x” marks indicate the integration limits used to extract the enthalpy of reaction.

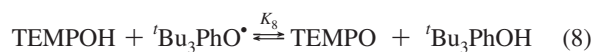
Inversion of the calorimeter mixed the solutions and initiated the reaction. The heat flux signal changes rapidly after the reaction is initiated and then gradually returns to its equilibrium value (Figure 2). Integration of this signal over the course of several hours gives the total heat released, which can be converted to ΔH° using the reagent concentrations. Both reagents started as solutions in order to avoid the contributions from the heat of solution for the solid reagent. Instead, the heats of dilution were measured, which are typically much smaller contributions to the overall heat flux.³⁴

The average of three measurements of the heat of reaction of $\text{Fe}^{\text{II}}(\text{H}_2\text{bip})$ and TEMPO (eq 4) gave $\Delta H^\circ_4 = -8.9 \pm 0.6$ kcal mol⁻¹. The observed heat of reaction was found to be independent of $[\text{TEMPO}]$, indicating that heat of dilution for TEMPO, $\Delta H^\circ_{\text{dil}}[\text{TEMPO}]$, is small. $\Delta H^\circ_{\text{dil}}[\text{Fe}^{\text{II}}(\text{H}_2\text{bip})]$ was measured independently and also found to be negligible. The value of ΔH°_4 from calorimetry is in excellent agreement with that determined previously from van't Hoff analysis of K_4 , -9.4

± 0.6 kcal mol⁻¹. Thus, calorimetry provides a direct and independent confirmation of the heat of reaction and also, because ΔG°_4 is well-known, the entropy of reaction, $\Delta S^\circ_4 = -30 \pm 2$ kcal mol⁻¹.

Attempts to measure other heats of metal HAT reactions unfortunately all proved problematic. For the reaction of **Fe^{III}(Hbim)** and TEMPOH, the exoergic direction for reaction 5, ¹H NMR and UV-vis spectra of product mixtures after calorimetric measurements showed decomposition of the iron product. This decomposition was found to be strongly exothermic and overwhelmed the small endothermic signal expected. The cobalt/TEMPO reaction (eq 3) is too slow to be reliably measured directly by the Calvet calorimeter apparatus, so the reaction of **Co^{II}(H₂bim)** with ^tBu₃PhO[•] was investigated instead. This reaction cleanly forms the HAT products **Co^{III}(Hbim)** and ^tBu₃PhOH over the few minutes required for kinetic measurements. On the multiple-hour time scale of the calorimetry experiment, however, the UV-vis spectra showed further reaction of the excess ^tBu₃PhO[•]. This further reactivity results in calorimetric molar reaction enthalpy values that vary linearly with the amount of excess ^tBu₃PhO[•] present, and this heat signal masks the enthalpy of the simple HAT reaction. Conditions with stoichiometric reagents or with excess **Co^{II}(H₂bim)** were also unsuccessful. Calorimetric measurements of the reactions of **Ru^{II}(py-imH)** with TEMPO (eq 6) or ^tBu₃PhO[•] gave irreproducible heat flux signals, with large shifts in the baseline heat flux before and after mixing. Similar baseline shifts were also observed in the heat of dilution of **Ru^{II}(py-imH)** experiments. These experiments unfortunately have to be run at the edge of the sensitivity of the calorimeter due to the low solubility of **Ru^{II}(py-imH)** in MeCN.

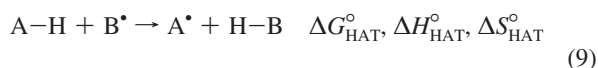
As part of these studies, the heat of H-atom transfer from TEMPOH to ^tBu₃PhO[•] to form TEMPO + ^tBu₃PhOH was measured (eq 8). These products are quantitatively formed and



the product mixture is stable overnight at 30 °C according to ¹H NMR and UV-vis spectra. The directly measured heats of dilution in MeCN ($\Delta H^\circ_{\text{dil}}$) for both TEMPOH and ^tBu₃PhO[•] are small, on the order of 2% of the total heat for the HAT reaction. The average of three experiments gave $\Delta H^\circ_8[\text{calorimetry}] = -11.2 \pm 0.5$ kcal mol⁻¹.

3. Discussion

3.1. Overview of Hydrogen Atom Transfer Thermochemistry. Hydrogen atom transfer (HAT^{11,29}) reactions in solution (eq 9) can be written as the sum of two *pseudo*-half-reactions, eqs 10 and 11. This is analogous to describing an electron transfer (ET) process as two ET half-reactions, except that in HAT these are complete reactions since they are not relative to a reference electrode. For HAT, each half-reaction is the definition of the bond dissociation enthalpy (BDE) or bond dissociation free energy (BDFE). Strictly speaking, BDEs and BDFEs are gas-phase quantities but it is convenient to consider analogues in solution, BDE_s and BDFE_s in solvent “s”. The driving force for eq 9 is therefore the difference between the BDFEs (or BDEs if working with enthalpy) of the two half-reactions, eq 12.



$$\Delta G^\circ_{\text{HAT},s} = \text{BDFE}[\text{AH}]_s - \text{BDFE}[\text{BH}]_s \quad (12)$$

$$\text{BDFE}[\text{AH}]_s = \text{BDE}[\text{AH}]_s - T\Delta S^\circ_s \quad (13)$$

$$\Delta S^\circ_s = S^\circ[\text{H}^\bullet]_s + S^\circ[\text{A}^\bullet]_s - S^\circ[\text{AH}]_s \quad (14)$$

$$S^\circ[\text{AH}]_s = S^\circ[\text{AH}]_g + \Delta S^\circ_{\text{solv}}[\text{AH}]_s \quad (15)$$

The BDFE_s and BDE_s are related by the entropy of reaction ΔS°_s (eq 13), which is the difference between absolute entropies of the component species in solution (eq 14). $S^\circ[\text{AH}]_s$ is the sum of the gas-phase entropy of AH ($S^\circ[\text{AH}]_g$) and the entropy of solvation of AH_g ($\Delta S^\circ_{\text{solv}}[\text{AH}]_s$), eq 15. Analogous definitions apply to $S^\circ[\text{H}^\bullet]_s$ and $S^\circ[\text{A}^\bullet]_s$. $S^\circ[\text{AH}]_g$ has contributions from the entropy of translations (depending on mass), rotations (depending on moment of inertia), vibrations (depending on frequencies), and electron spins.³⁷ $\Delta S^\circ_{\text{solv}}[\text{AH}]_s$ will vary given the polarity and hydrogen-bonding ability of the solvent used.³⁸

Organic HAT reactions, as noted above, have for many decades been analyzed using BDEs and the Bell-Evans-Polanyi (BEP) correlation of activation energies with $\Delta H^\circ_{\text{HAT}}$.^{1a,17,39} The differences between the BEP enthalpy treatment and more typical linear free-energy relationships (LFERs)^{18,19} have not previously been of serious concern because HAT reactions have typically been assumed to have ΔS°_s close to zero.²⁶ This assumption derives from the parallel assumption that (for most species) AH and A[•] have similar absolute entropies (eq 16) because they have similar mass, size, and charge. As discussed elsewhere, eq 16 appears to hold for small gas phase molecules and for solution phase organic compounds^{26,27} but does not hold for reactions of **Fe^{II}(H₂bip)**, **Fe^{II}(H₂bim)**,²⁸ and (as reported here) **Co^{II}(H₂bim)**.

$$S^\circ[\text{AH}]_s \approx S^\circ[\text{A}^\bullet]_s \quad (16)$$

The magnitude of $\Delta S^\circ_{\text{HAT}}$ has not been extensively explored for transition metal complexes.⁴⁰ The four different transition metal hydrogen atom donors studied here allow us to study the metal-based trends associated with ground-state entropies and to determine if a large $\Delta S^\circ_{\text{HAT}}$ is a general phenomenon for transition metal complexes.

3.2. Bond Dissociation Enthalpies and Free Energies. TEMPOH/TEMPO and ^tBu₃PhOH/^tBu₃PhO[•] are convenient and common hydrogen atom transfer reagents, and they are reference points for much of the thermochemistry described here. It is therefore important to assess the “best” current values for their O-H BDFEs and BDEs, as is done in the following sections and summarized in Table 2. In addition, the excellent agreement among the different approaches to these values supports the validity of each method.

3.2.1. Solution BDEs of ^tBu₃PhOH from Calorimetry. The literature on gas phase and solution phase BDEs of phenols is extensive.⁴¹ Data are available in a variety of solvents, and it is important in comparisons and thermochemical cycles to use

(38) Lynden-Bell, R. M.; Rasaiah, J. C. *J. Chem. Phys.* **1997**, *107*, 1981–1991.

(39) McMillen, D. F.; Golden, D. M. *Annu. Rev. Phys. Chem.* **1982**, *33*, 493–532.

Table 2. Bond Dissociation Free Energies (BDFEs) and Enthalpies (BDEs) in MeCN

AH	BDE _{MeCN} (kcal mol ⁻¹)	BDFE _{MeCN} (kcal mol ⁻¹)	Reference
^t Bu ₃ PhOH	83 ± 1	77 ± 1	see text, 34
TEMPOH	71.5 ± 0.5	66.5 ± 0.5	see text, 23, 35
Fe^{II}(H₂bip)	62.0 ± 1.7 ^a	66.0 ± 1.7 ^b	28, 30
Fe^{II}(H₂bim)	67 ± 2 ^a	72 ± 2 ^b	36
Ru^{II}(py-imH)	68 ± 1 ^a	62 ± 1 ^b	32
Ru ^{II} (hfac) ₂ (py-imH)	--	79.6 ± 1 ^b	32
Co^{II}(H₂bim)	62 ± 1 ^{a,c}	69.5 ± 0.9 ^c	see text

^a BDE_{MeCN} = ΔH^o_(AH + TEMPO) - BDE[TEMPOH]_{MeCN}. ^b From eq 21 using pK_a and E^o values. ^c From K_{eq} and ΔH^o values in Table 1; these are in agreement with values calculated from eq 21 (using pK_a and E^o), which are less precise for **Co^{II}(H₂bim)** because of the large uncertainty in E^o.³⁰

values in the same solvent.⁴² In 1969, calorimetry determined the heat of transfer of two H-atoms from diphenylhydrazine to 2 ^tBu₃PhO[•] in both benzene and CCl₄.³⁴ When coupled with the known solution heats of formation for PhNHNHPh and PhNNPh (the latter having been re-evaluated since 1969),⁴³ this gives ΔH^o_f[^tBu₃PhO[•]]_s - ΔH^o_f[^tBu₃PhOH]_s (28.09 ± 0.08 and 28.01 ± 0.12 kcal mol⁻¹ for C₆H₆ and CCl₄, respectively), which can be converted to a BDE_s using eq 17.

$$\text{BDE}_s = \Delta H_f^\circ[\text{A}^\bullet]_s - \Delta H_f^\circ[\text{AH}]_s + \Delta H_f^\circ[\text{H}^\bullet]_s \quad (17)$$

The last term in eq 17, ΔH^o_f[H[•]]_s, is the sum of the gas-phase heat of formation of H[•] (ΔH^o_f[H[•]]_g = 52.103 ± 0.001 kcal mol⁻¹)⁴⁴ and its enthalpy of solvation (ΔH^o_{solv}[H[•]]_s). The solvation of H₂ is considered to be a good model for solvation of H[•]⁴⁵ so ΔH^o_{solv}[H[•]]_s can be approximated by ΔH^o_{solv}[H₂]_s. ΔH^o_{solv}[H₂]_s values in benzene and CCl₄ are not known but should be similar to those in toluene and 1,2-dichloroethane (1.38 and 1.81 kcal mol⁻¹, respectively).^{46,47} Using these values in eq 17 gives solution BDEs for ^tBu₃PhOH of 81.6 ± 0.4 kcal mol⁻¹ in benzene and 82.0 ± 0.5 kcal mol⁻¹ in CCl₄.

- (40) (a) Wayner, D. D. M.; Parker, V. D. *Acc. Chem. Res.* **1993**, *26*, 287–294, and references therein. (b) Tang, L.; Papish, E. T.; Abramo, G. P.; Norton, J. R.; Baik, M. H.; Friesner, R. A.; Rappe, A. *J. Am. Chem. Soc.* **2003**, *125*, 10093–10102, and **2006**, *128*, 11314.
- (41) (a) dos Santos, R. M. B.; Cabral, B. J. C.; Simoes, J. A. M. *Pure Appl. Chem.* **2007**, *79*, 1369–1382. (b) Mulder, P.; Korth, H.-G.; Pratt, D. A.; DiLabio, G. A.; Valgimigli, L.; Pedulli, G. F.; Ingold, K. U. *J. Phys. Chem. A* **2005**, *109*, 2647–2655. (c) dos Santos, R. M. B.; Simoes, J. A. M. *J. Phys. Chem. Ref. Data* **1998**, *27*, 707–739.
- (42) One reason that the BDE[PhOH]_{soln} is still being debated in the literature revolves around the magnitude of solvation energies in different solvents and how best to interconvert between them. These effects are potentially magnified when dealing with transition metal complexes because of the increased polarity changes between oxidation states.
- (43) Pratt, D. A.; Blake, J. A.; Mulder, P.; Walton, J. C.; Korth, H.-G.; Ingold, K. U. *J. Am. Chem. Soc.* **2004**, *126*, 10667–10675.
- (44) *NIST Chemistry WebBook*. NIST Standard Reference Database 69; Linstrom, P. J., Mallard, W., Eds.; National Institute of Standards and Technology: Gaithersburg, MD 20899, June 2005.
- (45) (a) Parker, V. D. *J. Am. Chem. Soc.* **1992**, *114*, 7458–7462, and correction *J. Am. Chem. Soc.* **1993**, *115*, 1201. (b) Roduner, E. *Radiat. Phys. Chem.* **2005**, *72*, 201–206. (c) Roduner, E.; Bartels, D. M. *Ber. Bunsen-Ges. Phys. Chem.* **1992**, *96*, 1037–1042. It should be noted that the conversion between standard states in refs 45b and 45c do not correctly account for the unit mol fraction standard state in solution or the conversion between 1 atm and 1 M standard states in the gas phase.
- (46) Using ΔH^o_{solv}[H[•]]_s ≅ ΔH^o_{solv}[H₂]_s, ΔH^o_{solv}[H[•]]_s = 1.56, 1.38, and 1.81 kcal mol⁻¹ for MeCN, toluene, and ClCH₂CH₂Cl, respectively. ΔG^o_{solv}[H[•]]_{MeCN} ≅ ΔG^o_{solv}[H₂]_{MeCN} = 5.12 kcal mol⁻¹: Brunner, E. *J. Chem. Eng. Data* **1985**, *30*, 269–273.
- (47) *Hydrogen and Deuterium*; Young, L. C., Ed.; Pergamon Press: New York, 1981; Vol. 5/6.

The BDE of ^tBu₃PhOH in MeCN differs from the values in benzene and CCl₄ by the differences in solvation (eq 18). For H[•], the difference in solvation between benzene and MeCN is very small, 0.18 kcal mol⁻¹.⁴⁶ Ingold and co-workers have proposed that the difference in solvation between a phenol and

$$\begin{aligned} \text{BDE}_{s1} - \text{BDE}_{s2} &= \Delta H_{\text{solv}}^\circ[\text{A}^\bullet]_{s1} - \Delta H_{\text{solv}}^\circ[\text{AH}]_{s1} + \\ &\Delta H_{\text{solv}}^\circ[\text{H}^\bullet]_{s1} - (\Delta H_{\text{solv}}^\circ[\text{A}^\bullet]_{s2} - \Delta H_{\text{solv}}^\circ[\text{AH}]_{s2} + \Delta H_{\text{solv}}^\circ[\text{H}^\bullet]_{s2}) \end{aligned} \quad (18)$$

its radical is due primarily to differences in hydrogen bonding to the solvent^{41b} which they estimate using Abraham's empirical hydrogen-bond strength model.^{48,49} For AH = ^tBu₃PhOH, the Ingold/Abraham H-bonding model estimates {ΔH^o_{solv}[A[•]]_{MeCN} - ΔH^o_{solv}[AH]_{MeCN}} - {ΔH^o_{solv}[A[•]]_{C₆H₆} - ΔH^o_{solv}[AH]_{C₆H₆}} ≈ 1.3 kcal mol⁻¹,⁵⁰ and therefore BDE[^tBu₃PhOH]_{MeCN} = 83 ± 1 kcal mol⁻¹.

3.2.2. BDE and BDFE of ^tBu₃PhOH in MeCN from Gas Phase Data. The BDE_{MeCN} and BDFE_{MeCN} for ^tBu₃PhOH can also be determined from gas phase values and estimates for the appropriate solvation terms (eqs 18, 19). The gas phase BDE of ^tBu₃PhOH has been critically reviewed^{41c} and found to be 8.8 ± 0.95 kcal mol⁻¹ weaker than BDE[PhOH]_g, which is 88.7 ± 0.5 kcal mol⁻¹.^{41a} Therefore, the BDE[^tBu₃PhOH]_g = 79.9 ± 1.1 kcal mol⁻¹.

$$\text{BDE}[\text{AH}]_s = \text{BDE}[\text{AH}]_g + \Delta H_{\text{solv}}^\circ[\text{A}^\bullet]_s - \Delta H_{\text{solv}}^\circ[\text{AH}]_s + \Delta H_{\text{solv}}^\circ[\text{H}^\bullet]_s \quad (19)$$

$$\text{BDFE}[\text{AH}]_s = \text{BDFE}[\text{AH}]_g + \Delta G_{\text{solv}}^\circ[\text{A}^\bullet]_s - \Delta G_{\text{solv}}^\circ[\text{AH}]_s + \Delta G_{\text{solv}}^\circ[\text{H}^\bullet]_s \quad (20)$$

ΔH^o_{solv}[^tBu₃PhO[•]]_{MeCN} - ΔH^o_{solv}[^tBu₃PhOH]_{MeCN} has been estimated by two methods. The Ingold/Abraham H-bond model gives 1.43 kcal mol⁻¹.⁴⁹ Alternatively, ΔH^o_{solv}[^tBu₃PhO[•]]_{MeCN} - ΔH^o_{solv}[^tBu₃PhOH]_{MeCN} can be evaluated computationally. Bakalbassis et al. found that chemically accurate values of BDEs for several phenols could be obtained with the (RO)B3LYP level of theory using a nonstandard basis set (see Experimental Section for details).⁵¹ In our laboratory, this method yields BDE[^tBu₃PhOH]_{g,DFT} = 79.3 kcal mol⁻¹, in good agreement with the experimental value above. Application of a polarizable continuum solvation model (PCM) yields the slightly negative value for ΔH^o_{solv}[^tBu₃PhO[•]]_{MeCN} - ΔH^o_{solv}[^tBu₃PhOH]_{MeCN} of -0.4 kcal mol⁻¹. This is a consequence of the larger dipole

- (48) (a) Abraham, M. H.; Grellier, P. L.; Prior, D. V.; Duce, P. P.; Morris, J. J.; Taylor, P. J. *J. Chem. Soc., Perkin Trans. 2* **1989**, 699–711. (b) Abraham, M. H.; Grellier, P. L.; Prior, D. V.; Morris, J. J.; Taylor, P. J. *J. Chem. Soc., Perkin Trans. 2* **1990**, 521–529. (c) Abraham, M. H.; Grellier, P. L.; Prior, D. V.; Taft, R. W.; Morris, J. J.; Taylor, P. J.; Laurence, C.; Berthelot, M.; Doherty, R. M.; Kamlet, M. J.; Abboud, J.-L. M.; Sraidi, K.; Guihéneuf, G. *J. Am. Chem. Soc.* **1988**, *110*, 8534–8536. (d) Abraham, M. H.; Platts, J. A. *J. Org. Chem.* **2001**, *66*, 3484–3491. (e) This model is parameterized into the acidity (α^H₂) and the basicity (β^H₂) of the hydrogen bond donor and acceptor.
- (49) A review of several solvation models for PhOH^{41a} suggests that the Ingold/Abraham H-bonding model is an overestimate of (ΔH^o_{solv}[A[•]]_s - ΔH^o_{solv}[AH]_s).
- (50) From ref 41b: ΔH^o_{solv}[A[•]]_{MeCN} - ΔH^o_{solv}[AH]_{MeCN} - (ΔH^o_{solv}[A[•]]_{C₆H₆} - ΔH^o_{solv}[AH]_{C₆H₆}) ≈ -χ_{Hbond} × ΔH^o_{Hbond,MeCN} + χ_{Hbond} × ΔH^o_{Hbond,C₆H₆}. χ_{Hbond} is the fraction of hydrogen-bonded species in solution and log K_{Hbond} = 7.354 × α^H_{2,AH} × β^H_{2,solvent} - 1.094. From Litwinienko, G.; Ingold, K. U. *J. Org. Chem.* **2003**, *68*, 3433–3438, and ref 48b: α^H₂(^tBu₃PhOH) = 0.24, β^H₂(MeCN) = 0.44, β^H₂(benzene) = 0.14.
- (51) Bakalbassis, E. G.; Lithoxidou, A. T.; Vafiadis, A. P. *J. Phys. Chem. A* **2003**, *107*, 8594–8606.

moment of ${}^t\text{Bu}_3\text{PhO}^\bullet$. Together, eq 19, the BDE $[\text{}^t\text{Bu}_3\text{PhOH}]_g$ of 79.9 kcal mol $^{-1}$, and the average of the two solvation models above (0.5 ± 1.3 kcal mol $^{-1}$) give BDE $[\text{}^t\text{Bu}_3\text{PhOH}]_{\text{MeCN}} = 82 \pm 2$ kcal mol $^{-1}$, consistent with the independently determined calorimetric value above.

The bond dissociation free energy for ${}^t\text{Bu}_3\text{PhOH}$ can also be determined using eq 20, starting with BDFE $[\text{}^t\text{Bu}_3\text{PhOH}]_g = 71.8 \pm 1$ kcal mol $^{-1}$.⁵² As above, PCM calculations were used to compute $\Delta G^\circ_{\text{sol}}[\text{}^t\text{Bu}_3\text{PhO}^\bullet]_{\text{MeCN}} - \Delta G^\circ_{\text{sol}}[\text{}^t\text{Bu}_3\text{PhOH}]_{\text{MeCN}} = -0.4$ kcal mol $^{-1}$ (see Experimental Section for details). Ingold's model gives similarly small values. When used in eq 20, with $\Delta G^\circ_{\text{sol}}[\text{H}^\bullet]_{\text{MeCN}} \cong \Delta G^\circ_{\text{sol}}[\text{H}_2]_{\text{MeCN}} = 5.12$ kcal mol $^{-1}$,⁴⁶ the BDFE $[\text{}^t\text{Bu}_3\text{PhOH}]_{\text{MeCN}}$ is 77 ± 1 kcal mol $^{-1}$.

3.2.3. BDFE of ${}^t\text{Bu}_3\text{PhOH}$ in MeCN from pK_a and E° Measurements. An alternative measure of BDFE $_{\text{MeCN}}$ is obtained from a thermochemical cycle using a pK_a and an E° (eq 21).

$$\text{BDFE}_{\text{MeCN}}(\text{kcal mol}^{-1}) = nFE^\circ(\text{vsFc}^{+/0}) + 2.303RTpK_a + 54.9 \quad (21)$$

Bordwell and co-workers popularized the method in DMSO,²² and Tilset worked out the cycle for MeCN.²⁰ The two reported values for $E^\circ[\text{}^t\text{Bu}_3\text{PhO}^\bullet]$ in MeCN vs $\text{Cp}_2\text{Fe}^{+/0}$, -707 ⁵³ and -689 mV,⁵⁴ averaged to -0.70 V. The pK_a in DMSO for ${}^t\text{Bu}_3\text{PhOH}$ (17.8)⁵⁵ can be converted into a value of 27.5 in MeCN using the linear relationship found by Kutt and co-workers.⁵⁶ Putting these values into eq 21 gives BDFE $[\text{}^t\text{Bu}_3\text{PhOH}]_{\text{MeCN}} = 76 \pm 1.3$ kcal mol $^{-1}$. The measured equilibrium constant for reaction of ${}^t\text{Bu}_3\text{PhO}^\bullet$ with $\text{Ru}^{\text{II}}(\text{hfac})_2(\text{py-imH})$, eq 7 above, provides another measure of BDFE $[\text{}^t\text{Bu}_3\text{PhOH}]_{\text{MeCN}}$, since the BDFE of the ruthenium complex is known from its pK_a and an E° values.³² Application of eq 12 to these data gives a BDFE $[\text{}^t\text{Bu}_3\text{PhOH}]_{\text{MeCN}}$ of 78 ± 1 kcal mol $^{-1}$. The close agreement among these three BDFE values (77 ± 1 , 76 ± 1 , and 78 ± 1 kcal mol $^{-1}$) supports the validity of all three approaches and indicates a consensus BDFE $[\text{}^t\text{Bu}_3\text{PhOH}]_{\text{MeCN}}$ of 77 ± 1 kcal mol $^{-1}$ (Table 2).

3.2.4. BDFE and BDE of TEMPOH in MeCN. A calorimetric study of the reaction of TEMPO with diphenylhydrazine in benzene,³⁵ following the analysis above for ${}^t\text{Bu}_3\text{PhOH}$, gives⁵⁷ BDE $[\text{TEMPOH}]_{\text{C}_6\text{H}_6} = 70.0 \pm 0.8$ kcal mol $^{-1}$ and BDE $[\text{TEMPOH}]_{\text{MeCN}} = 71.5 \pm 0.9$ kcal mol $^{-1}$. This BDE can be converted to a BDFE of 66.4 ± 0.5 kcal mol $^{-1}$ via eqs 13 and 14 assuming

(52) (a) Calculated from BDFE $[\text{}^t\text{Bu}_3\text{PhOH}]_g = \text{BDE}[\text{}^t\text{Bu}_3\text{PhOH}]_g - T(S^\circ[\text{H}^\bullet]_g + S^\circ[\text{}^t\text{Bu}_3\text{PhO}^\bullet]_g - S^\circ[\text{}^t\text{Bu}_3\text{PhOH}]_g)$. $S^\circ[\text{H}^\bullet]_g = 27.419$ cal mol $^{-1}$ K $^{-1}$.⁴⁴ $S^\circ[\text{}^t\text{Bu}_3\text{PhO}^\bullet]_g - S^\circ[\text{}^t\text{Bu}_3\text{PhOH}]_g$ is assumed to be negligible based on the small values of the related entropies of formation $\{S^\circ[\text{benzyl radical}]_g - S^\circ[\text{toluene}]_g\}$ and $\{S^\circ[\text{PhO}^\bullet]_g - S^\circ[\text{PhOH}]_g\}$ (-0.47 and -0.8 cal mol $^{-1}$ K $^{-1}$). Entropies of formation from refs 52b–e. (b) Curran, H.; Wu, C.; Marinov, N.; Pitz, W. J.; Westbrook, C. K.; Burcat, A. *J. Phys. Chem. Ref. Data* **2000**, *29*, 463–517. (c) Ruscic, B.; Boggs, J. E.; Burcat, A.; Csaszar, A. G.; Demaison, J.; Janoschek, R.; Martin, J. M. L.; Morton, M. L.; Rossi, M. J.; Stanton, J. F.; Szalay, P. G.; Westmoreland, P. R.; Zabel, F.; Berces, T. *J. Phys. Chem. Ref. Data* **2005**, *34*, 573–656. (d) Burcat, A.; Ruscic, B. TAE Report No. 960; Technical Report, 2005. (e) See also ftp://ftp.technion.ac.il/pub/supported/aetdd/thermodynamics.

(53) Niyazymbetov, M. E.; Evans, D. H. *J. Chem. Soc., Perkin Trans. 2* **1993**, *7*, 1333–1338.

(54) Grampp, G.; Landgraf, S.; Muresanu, C. *Electrochim. Acta* **2004**, *49*, 537–544. This value was reported vs SCE and converted to vs $\text{Cp}_2\text{Fe}^{+/0}$ by adding $+0.4$ V. Connelly, N. G.; Geiger, W. E. *Chem. Rev.* **1996**, *96*, 877–910.

(55) Bordwell, F. G.; Cheng, J.-P. *J. Am. Chem. Soc.* **1991**, *113*, 1736–1743.

(56) Kutt, A.; Leito, I.; Kaljurand, I.; Soovali, L.; Vlasov, V. M.; Yagupolskii, L. M.; Koppel, I. A. *J. Org. Chem.* **2006**, *71*, 2829–2838.

that $S^\circ[\text{TEMPO}]_{\text{MeCN}} \approx S^\circ[\text{TEMPOH}]_{\text{MeCN}}$ (an example of eq 16) and $\Delta G^\circ_{\text{sol}}[\text{H}^\bullet]_{\text{MeCN}} = 5.12$ kcal mol $^{-1}$. This BDFE $[\text{TEMPOH}]_{\text{MeCN}}$ can also be calculated directly using the known pK_a and E° values (eq 21), which gives 66.9 ± 0.5 kcal mol $^{-1}$ (see Supporting Information). BDFE $[\text{TEMPOH}]_{\text{MeCN}}$ is also determined by the equilibrium constants for reactions of $\text{Fe}^{\text{II}}(\text{H}_2\text{bip})$,²⁸ $\text{Fe}^{\text{II}}(\text{H}_2\text{bim})$,²⁸ or $\text{Ru}^{\text{II}}(\text{py-imH})$ ³² with TEMPO (the BDFEs for each metal complex independently determined from pK_a and E° values). The average value from these equilibration experiments, 66.5 ± 0.5 kcal mol $^{-1}$, is essentially the same as the values from the TEMPOH pK_a and E° and from calorimetry. This agreement supports the consensus BDFE value (Table 2) and the assumption that $S^\circ[\text{TEMPO}]_{\text{MeCN}} \approx S^\circ[\text{TEMPOH}]_{\text{MeCN}}$.

3.2.5. Solution BDFE and BDE of Metal Complexes in MeCN. For each of the four metal complexes examined here, the BDFE $_{\text{MeCN}}$ was determined using eq 21 and the relevant pK_a and E° values (which have been previously reported^{32,30}). As noted above, these values are consistent with the measured equilibrium constants and the BDFEs of TEMPOH and ${}^t\text{Bu}_3\text{PhOH}$. The BDE $_{\text{MeCN}}$ (enthalpies) shown in Table 2 were calculated from the BDFE $_{\text{MeCN}}$ values and the experimentally determined $\Delta S^\circ_{\text{MeCN}}$ for reaction with TEMPO, attributing all of this ΔS° to the metal complex “half-reaction” (eq 11).

3.3. Comparison between Calorimetry and van't Hoff Methodologies. The calorimetric experiments confirm the enthalpy of reaction of $\text{Fe}^{\text{II}}(\text{H}_2\text{bip}) + \text{TEMPO}$ (eq 4) measured by solution equilibrium and kinetic data. The $\Delta H^\circ_4[\text{calorimetry}] = -8.9 \pm 0.6$ kcal mol $^{-1}$ is within error of $\Delta H^\circ_4[\text{van't Hoff}] = -9.4 \pm 0.6$ kcal mol $^{-1}$.²⁸ This quantitative agreement confirms the large negative $\Delta S^\circ_5 = -30 \pm 3$ cal mol $^{-1}$ K $^{-1}$.²⁸ Similarly, the calorimetric heat of H-atom transfer from TEMPOH to ${}^t\text{Bu}_3\text{PhO}^\bullet$ (eq 8), $\Delta H^\circ_8[\text{calorimetry}] = -11.2 \pm 0.5$ kcal mol $^{-1}$, agrees with the value calculated from the literature solution BDEs in MeCN (Table 2), -11.5 ± 1.4 kcal mol $^{-1}$. Calorimetric studies of $\text{Ru}^{\text{II}}(\text{py-imH})$, $\text{Fe}^{\text{III}}(\text{Hbim})$, and $\text{Co}^{\text{II}}(\text{H}_2\text{bim})$ plus TEMPO were unsuccessful because the reactions did not meet the experimental requirements of high solubilities and good long-term stability of the reaction mixtures. For these systems, the van't Hoff methodology is easier and more reliable for determining the ground-state thermodynamics, as long as equilibrium constants are measurable.

3.4. Origins of the ΔS° for H-Atom Transfer. The four reactions of transition metal H-atom donors with the same atom acceptor, TEMPO, have widely varying values of ΔS° (Table 1). The reaction of $\text{Ru}^{\text{II}}(\text{py-imH})$ shows only a small positive entropy, $\Delta S^\circ_6 = 4.9$ cal mol $^{-1}$ K $^{-1}$. The reactions with $\text{Fe}^{\text{II}}(\text{H}_2\text{bip})$, $\text{Fe}^{\text{II}}(\text{H}_2\text{bim})$, $\text{Co}^{\text{II}}(\text{H}_2\text{bim})$ show much larger negative values: $\Delta S^\circ_{\text{HAT}} = -30$, -30 , and -41 cal mol $^{-1}$ K $^{-1}$, respectively. These are very substantial values of $|\Delta S^\circ_{\text{HAT}}|$, in contradiction with the common assumption that the entropic contribution to HAT is not significant. Thinking of these reactions as the sum of two quasi-half-reactions (eqs 9–11), $\Delta S^\circ_{\text{HAT}} \neq 0$ requires that $S^\circ[\text{AH}]_s \neq S^\circ[\text{A}^\bullet]_s$ (in contradiction to eq 16) for either the metal or organic redox couple.

The independent measurements of the BDE $_{\text{MeCN}}$ and the BDFE $_{\text{MeCN}}$ in Section II give (after subtracting $T S^\circ[\text{H}^\bullet]_{\text{MeCN}}$) $\{S^\circ[\text{TEMPO}]_{\text{MeCN}} - S^\circ[\text{TEMPOH}]_{\text{MeCN}}\} = 1 \pm 4$ cal mol $^{-1}$ K $^{-1}$ and $\{S^\circ[\text{}^t\text{Bu}_3\text{PhO}^\bullet]_{\text{MeCN}} - S^\circ[\text{}^t\text{Bu}_3\text{PhOH}]_{\text{MeCN}}\} = 5 \pm 7$ cal mol $^{-1}$ K $^{-1}$. In addition, HAT from TEMPOH to ${}^t\text{Bu}_3\text{PhO}^\bullet$ (eq 8) has $\Delta H^\circ_8 = -11.2 \pm 0.5$ kcal mol $^{-1}$ and $\Delta G^\circ_8 = -10.5 \pm 1.3$ kcal mol $^{-1}$ so $\Delta S^\circ_8 = -2 \pm 3$ cal mol $^{-1}$ K $^{-1}$. The difference between ΔS°_8 and $\{S^\circ[\text{TEMPO}]_{\text{MeCN}} - S^\circ[\text{TEMPOH}]_{\text{MeCN}}\}$

further limits the entropy for $\{S^\circ[\text{Bu}_3\text{PhO}^+]\}_{\text{MeCN}} - S^\circ[\text{Bu}_3\text{PhOH}]\}_{\text{MeCN}}$ to $3 \pm 5 \text{ cal mol}^{-1} \text{ K}^{-1}$. These data demonstrate that $S^\circ[\text{AH}]_s - S^\circ[\text{A}^+]_s \approx 0$ for both TEMPOH and Bu_3PhOH . Therefore, the unusual entropy contributions in our HAT reactions come from the metal redox couple.

The metal redox couples for reactions 3–6 show the following trend for $|\Delta S^\circ|$: $\text{Ru}^{\text{II}}(\text{py-imH}) \ll \text{Fe}^{\text{II}}(\text{H}_2\text{bip}) \approx \text{Fe}^{\text{II}}(\text{H}_2\text{bim}) < \text{Co}^{\text{II}}(\text{H}_2\text{bim})$. The Fe and Co reactions have negative entropies, indicating that the $\text{M}^{\text{III}}(\text{HL})$ complex is more ordered than $\text{M}^{\text{II}}(\text{H}_2\text{L})$. For the iron systems, previous experimental and computational studies²⁸ showed that the large $|\Delta S^\circ|$ originates primarily from changes in the vibrational entropy ($\Delta S^\circ_{\text{vib}}$) upon oxidation of the iron. The calculations showed that the primary contributors are *ca.* 30 low-frequency ($\nu \leq kT = 207 \text{ cm}^{-1}$ at 298 K) torsions and bends that change frequency between the Fe^{II} and Fe^{III} compounds.²⁸ Alternative origins of the large $|\Delta S^\circ|$ such as ion pairing or solvent effects were ruled out.

For $\text{Co}^{\text{II}}(\text{H}_2\text{bim}) + \text{TEMPO}$, the $\Delta S^\circ_{\text{HAT}} (-41 \pm 2 \text{ cal mol}^{-1} \text{ K}^{-1})$ is even more negative than that for the two iron reactions. In solution, $\text{Co}^{\text{II}}(\text{H}_2\text{bim})$ is entirely high-spin, while $\text{Co}^{\text{III}}(\text{H-bim})$ is entirely low-spin.³¹ In the idealized octahedral case, this is a change in multiplicity from a 12-fold degenerate ${}^4\text{T}_{1g}$ Co^{II} electronic state to a nondegenerate ${}^1\text{A}_{1g}$ Co^{III} state, an electronic entropy of $R \ln(12)$ or $\Delta S^\circ_{\text{elec}} = -4.9 \text{ cal mol}^{-1} \text{ K}^{-1}$. This maximum value of $\Delta S^\circ_{\text{elec}}$ (spin–orbit coupling and the D_3 symmetry of $\text{Co}^{\text{II}}(\text{H}_2\text{bim})$ will lower the degeneracy) is still a minor contribution to the observed $\Delta S^\circ_{\text{HAT}}$. The Co and Fe complexes are very similar in structure (in both systems the M–N bond lengths are $\sim 0.1 \text{ \AA}$ shorter in the M^{III} derivative),^{31,36} in acidity (similar pK_a values in MeCN); and in hydrogen bonding (the ΔG° for formation of a hydrogen-bonded adduct between TEMPOH and either $\text{Co}^{\text{III}}(\text{Hbim})$ or $\text{Fe}^{\text{III}}(\text{Hbim})$ differs by less than $0.1 \text{ kcal mol}^{-1}$).^{28,58} This similarity suggests a common vibrational origin for the entropy in both systems. The entropy would be expected to be larger for Co, since the high-spin to low-spin conversion should cause even larger frequency changes.^{67,60a} An increase of *ca.* $10 \text{ cal mol}^{-1} \text{ K}^{-1}$ for the addition of a spin-change is not unreasonable based on the electron transfer entropies discussed below. The ruthenium complexes, with a $4d$ transition metal, are all low-spin and have stronger bonds and therefore fewer low-frequency vibrational modes. With fewer modes $\leq kT$, the vibrational entropy will be much reduced, as observed: $\text{Ru}^{\text{II}}(\text{py-imH}) + \text{TEMPOH}$ has $\Delta S^\circ_{\text{HAT}} = 4.9 \pm 1.1 \text{ cal mol}^{-1} \text{ K}^{-1}$. Thus the trend for $|\Delta S^\circ_{\text{HAT}}|$, $\text{Ru}^{\text{II}}(\text{py-imH}) \ll \text{Fe}^{\text{II}}(\text{H}_2\text{bip}) \approx \text{Fe}^{\text{II}}(\text{H}_2\text{bim}) < \text{Co}^{\text{II}}(\text{H}_2\text{bim})$, is consistent with a dominant role for vibrational entropy in these reactions.

3.5. Trends in Electron Transfer Entropies. The entropies of electron transfer half-reactions ($\Delta S^\circ_{\text{ET}}$, eq 22) have been determined for a wide range of complexes and found to depend on the nature of the metal center, the associated redox change, the coordinating ligands, and the surrounding solvent and counterions.^{59–65} We note that, by convention, the ET half-reaction in eq 22 is written as a reduction, opposite to the way the HAT reactions are written here (eqs 10, 11).



Vibrational entropy has been shown to be important in both electron transfer^{66,67} and spin-equilibrium processes,^{68,69} when there are changes in metal–ligand bonding upon redox or spin change. Richardson and Sharpe estimated that in the gas phase the vibrational contribution to the total electron transfer entropy ranges from as low as 9% in RuO_4 (where there are few vibrations and many are at high frequency) up to 42% in $[\text{Fe}(\text{CN})_6]^{4-}$.^{67a} Vibrational entropy is a substantial part of the measured $\Delta S^\circ_{\text{ET}} = 29 \pm 3 \text{ cal mol}^{-1} \text{ K}^{-1}$ for the $\text{Fe}^{\text{II}}(\text{H}_2\text{bim})/\text{Fe}^{\text{III}}(\text{H}_2\text{bim})$ redox couple²⁸ and of the $\Delta S^\circ_{\text{HAT}}$ observed for the HAT reactions of $\text{Fe}^{\text{II}}(\text{H}_2\text{bim})$ and $\text{Fe}^{\text{II}}(\text{H}_2\text{bip})$. These

- (57) The reported calorimetric value³⁵ for $\Delta H^\circ_f[\text{TEMPO} - \text{TEMPOH}]_{\text{C}_6\text{H}_6}$ of $16.52 \pm 0.5 \text{ kcal mol}^{-1}$ was corrected for the revised ΔH°_f of azobenzene.⁴³ The values of $\Delta H^\circ_f[\text{H}^+]_{\text{C}_6\text{H}_6}$ and $\Delta H^\circ_f[\text{H}^+]_{\text{MeCN}}$ are given above, and $S^\circ[\text{TEMPO}]_{\text{MeCN}}$ is taken as equal to $S^\circ[\text{TEMPOH}]_{\text{MeCN}}$ for the reasons given above.
- (58) Mader, E. A.; Mayer, J. M. In preparation.
- (59) (a) Turner, J. W.; Schultz, F. A. *J. Phys. Chem. B* **2002**, *106*, 2009–2017. (b) Turner, J. W.; Schultz, F. A. *Inorg. Chem.* **2001**, *40*, 5296–5298. (c) Sharpe, P.; Kebarle, P. *J. Am. Chem. Soc.* **1993**, *115*, 782–789. (d) Kratochvil, B.; Knoeck, J. *J. Phys. Chem.* **1966**, *70*, 944–946. (e) Hupp, J. T.; Weaver, M. J. *Inorg. Chem.* **1983**, *22*, 2557–2564. (f) Sahami, S.; Weaver, M. J. *J. Electroanal. Chem. Interfacial Electrochem.* **1981**, *122*, 155–170. (g) Hupp, J. T.; Weaver, M. J. *Inorg. Chem.* **1984**, *23*, 3639–3644. (h) Yee, E. L.; Weaver, M. J. *Inorg. Chem.* **1980**, *19*, 1077–1079.
- (60) (a) Turner, J. W.; Schultz, F. A. *Inorg. Chem.* **1999**, *38*, 358–364. (b) Sahami, S.; Weaver, M. J. *J. Electroanal. Chem. Interfacial Electrochem.* **1981**, *122*, 171–181.

- (61) (a) Lay, P. A.; McAlpine, N. S.; Hupp, J. T.; Weaver, M. J.; Sargeson, A. M. *Inorg. Chem.* **1990**, *29*, 4322–4328. (b) Koval, C. A.; Gustafson, R. M.; Reidsema, C. M. *Inorg. Chem.* **1987**, *26*, 950–952. (c) Moattar, F.; Walton, J. R.; Bennett, L. E. *Inorg. Chem.* **1983**, *22*, 550–553.
- (62) (a) Hupp, J. T.; Weaver, M. J. *Inorg. Chem.* **1984**, *23*, 256–258. (b) Ogino, H.; Ogino, K. *Inorg. Chem.* **1983**, *22*, 2208–2211.
- (63) Schmitz, J. E. J.; Van der Linden, J. G. M. *Inorg. Chem.* **1984**, *23*, 3298–3303.
- (64) Tabib, J.; Hupp, J. T.; Weaver, M. J. *Inorg. Chem.* **1986**, *25*, 1916–1918.
- (65) (a) Schmitz, J. E. J.; Van der Linden, J. G. M. *Inorg. Chem.* **1984**, *23*, 117–119. (b) Crawford, P. W.; Schultz, F. A. *Inorg. Chem.* **1994**, *33*, 4344–4350. (c) Gao, Y.-D.; Lipkowitz, K. B.; Schultz, F. A. *J. Am. Chem. Soc.* **1995**, *117*, 11932–11938. (d) Sharpe, P.; Kebarle, P. *J. Am. Chem. Soc.* **1993**, *115*, 782–789. (e) Ogino, H.; Nagata, T.; Ogino, K. *Inorg. Chem.* **1989**, *28*, 3656–3659. (f) Youngblood, M. P.; Margerum, D. W. *Inorg. Chem.* **1980**, *19*, 3068–3072. (g) Kadish, K. M.; Das, K.; Schaeper, D.; Merrill, C. L.; Welch, B. R.; Wilson, L. J. *Inorg. Chem.* **1980**, *19*, 2816–2821. (h) George, P.; Hanania, G. I. H.; Irvine, D. H. *Recl. Trav. Chim. Pays-Bas Belg.* **1956**, *75*, 759–762. (i) Blonk, H. L.; Roelofsen, A. M.; Frelink, T.; Anders, M. J.; Schmitz, J. E. J.; Van der Linden, J. G. M.; Steggerda, J. J. *J. Phys. Chem.* **1992**, *96*, 6004–6012. (j) Weaver, M. J.; Nettles, S. M. *Inorg. Chem.* **1980**, *19*, 1641–1646. (k) George, P.; Hanania, G. I. H.; Irvine, D. H. *J. Chem. Soc.* **1959**, 2548–2554. (l) Zhu, T.; Su, C. H.; Schaeper, D.; Lemke, B. K.; Wilson, L. J.; Kadish, K. M. *Inorg. Chem.* **1984**, *23*, 4345–4349. (m) Noviadri, I.; Brown, K. N.; Fleming, D. S.; Gulyas, P. T.; Lay, P. A.; Masters, A. F.; Phillips, L. *J. Phys. Chem. B* **1999**, *103*, 6713–6722. (n) Moulton, R.; Weidman, T. W.; Vollhardt, K. P. C.; Bard, A. J. *Inorg. Chem.* **1986**, *25*, 1846–1851. (o) Ryan, M. F.; Elyer, J. R.; Richardson, D. E. *J. Am. Chem. Soc.* **1992**, *114*, 8611–8619. (p) Fabbrizzi, L.; Mariani, M.; Seghi, B.; Zanchi, F. *Inorg. Chem.* **1989**, *28*, 3362–3366. (q) Fabbrizzi, L.; Perotti, A.; Profumo, A.; Soldi, T. *Inorg. Chem.* **1986**, *25*, 4256–4259. (r) Blackburn, R. L.; Hupp, J. T. *Inorg. Chem.* **1989**, *28*, 3786–3790. (s) Curtis, J. C.; Blackburn, R. L.; Ennix, K. S.; Hu, S.; Roberts, J. A.; Hupp, J. T. *Inorg. Chem.* **1989**, *28*, 3791–3795.
- (66) (a) Turner, J. W.; Schultz, F. A. *Coord. Chem. Rev.* **2001**, *219*–221, 81–97. (b) Goodwin, H. A. *Top. Curr. Chem.* **2004**, *233*, 59–90.
- (67) (a) Richardson, D. E.; Sharpe, P. *Inorg. Chem.* **1993**, *32*, 1809–1812. (b) Richardson, D. E.; Sharpe, P. *Inorg. Chem.* **1991**, *30*, 1412–1414.
- (68) (a) Sorai, M.; Seki, S. *J. Phys. Chem. Solids* **1974**, *35*, 555–570. (b) van Koningsbruggen, P. J.; Maeda, Y.; Oshio, H. *Top. Curr. Chem.* **2004**, *233*, 259–324. (c) Gutlich, P.; Goodwin, H. A. Spin crossover - An overall perspective. In *Spin Crossover in Transition Metal Compounds I*; Springer-Verlag Berlin: Berlin, 2004; Vol. 233, pp 1–47. (d) König, E. *Struct. Bonding (Berlin)* **1991**, *76*, 51–152.
- (69) Note that spin-crossover entropies are substantially larger than expected solely from the electronic multiplicities. For example, $\Delta S^\circ_{\text{elec}}$ is $-5.4 \text{ cal mol}^{-1} \text{ K}^{-1}$ for high-spin ${}^5\text{T}_{2g}$ Fe^{II} low-spin \rightleftharpoons ${}^1\text{A}_{1g}$ Fe^{II} , much less than the measured $\Delta S^\circ_{\text{SCO}} = -21 \text{ cal mol}^{-1} \text{ K}^{-1}$ for $\text{Fe}^{\text{II}}(\text{H}_2\text{bip})$.³¹

entropies are close in magnitude because they both arise from the Fe^{III} complexes being more rigid and having fewer low-frequency vibrational modes than Fe^{II}.²⁸ In general, when vibrational entropy is a significant contributor, there should be a strong parallel between the entropies for ET and HAT reactions in a given system.

Differences in electron transfer entropies between redox two couples, when measured in the same solvent for reagents of the same charge, are primarily due to vibrational and electronic entropies.^{60a} For example, $\{\Delta S_{\text{ET}}^{\circ}[\text{Co}(\text{tacn})_3]^{3+/2+}_{\text{solv}} - \Delta S_{\text{ET}}^{\circ}[\text{Ru}(\text{tacn})_3]^{3+/2+}_{\text{solv}}\}$ is $16 \pm 3 \text{ cal mol}^{-1} \text{ K}^{-1}$ for solv = DMSO, acetone, water, and four other solvents (tacn = 1,4,7-triazacyclononane).^{60a,70,71} This difference is independent of solvent because the electronic and vibrational entropies do not depend on the solvent. $\{\Delta S_{\text{vib}}^{\circ}[\text{Co}(\text{tacn})_3]^{3+/2+} - \Delta S_{\text{vib}}^{\circ}[\text{Ru}(\text{tacn})_3]^{3+/2+}\}$ has been estimated as $12.7 \text{ cal mol}^{-1} \text{ K}^{-1}$, and the remainder of the difference can be accounted for by $\Delta S_{\text{elec}}^{\circ}$.^{60a}

The results described in this report indicate that, when comparing one transition metal system to another, the same trends are observed in the half-reaction entropies for both $\Delta S_{\text{ET}}^{\circ}$ and $|\Delta S_{\text{HAT}}^{\circ}|$. The Co^{III}/Co^{II} couples have the largest $\Delta S_{\text{ET}}^{\circ}$, with the exception of a few lanthanide and actinide complexes,^{59d,64,72} because they involve a spin-state change (low-spin Co^{III} to high-spin Co^{II}) in addition to an oxidation state change. $\Delta S_{\text{ET}}^{\circ}$ for Co^{III}/Co^{II} couples ranges from 30 to 50 $\text{cal mol}^{-1} \text{ K}^{-1}$ in organic solvents.^{59f,60,61,67,72,73} For similar complexes, $\Delta S_{\text{ET}}^{\circ}$ values for Co derivatives are typically 10–20 $\text{cal mol}^{-1} \text{ K}^{-1}$ larger than those for the Fe analogues. In our measurements of HAT entropies, the Co reaction has the largest $|\Delta S_{\text{HAT}}^{\circ}|$ (ca. $-41 \text{ cal mol}^{-1} \text{ K}^{-1}$), 11 $\text{cal mol}^{-1} \text{ K}^{-1}$ more negative than the iron analogues in the same reaction with TEMPO. Fe^{III/II} couples have a $\Delta S_{\text{ET}}^{\circ}$ of typically 15–30 $\text{cal mol}^{-1} \text{ K}^{-1}$ in organic solvents (except for those with an accompanying spin change).^{59,60,67} Ru^{III/Ru} couples have $\Delta S_{\text{ET}}^{\circ}$ values in a similar range as Fe^{III/Fe} couples (~ 10 – $30 \text{ cal mol}^{-1} \text{ K}^{-1}$,^{59,60,66a,67,72}). When complexes in the same solvent are compared, low-spin Fe^{III/II} couples are quite similar to the Ru^{III/II} analogues, while iron couples that exhibit spin equilibrium or are high-spin only have larger $\Delta S_{\text{ET}}^{\circ}$ values than the related Ru^{III/II} couples (probably due to larger vibrational entropies).⁷⁴

Thus the trend for $\Delta S_{\text{ET}}^{\circ}$ is Co > high-spin Fe > low-spin Fe \approx Ru.^{59b} This is the same as the trend in $-\Delta S_{\text{HAT}}^{\circ}$ described above for HAT (recall that the half-reactions are by convention written in opposite directions for ET (eq 22) and HAT (eq 10), so the signs are opposite). This trend is a result of the major contribution of $\Delta S_{\text{vib}}^{\circ}$, for both HAT and ET reactions of transition metal complexes. The close connection between $\Delta S_{\text{ET}}^{\circ}$

and $\Delta S_{\text{HAT}}^{\circ}$ provides valuable insight in cases where only one or the other has been measured. In particular, it suggests that ground-state entropy effects will be important for HAT reactions of high-spin first-row transition metals.

3.6. Relevance to Biological Systems and HAT Analyses. The observation of significant ground-state entropies for HAT reactions appears to be general for first-row transition metal coordination complexes. This leads to a significant temperature dependence of ΔG . For instance, in a reaction with $\Delta S^{\circ} = -30 \text{ cal mol}^{-1} \text{ K}^{-1}$ such as observed for the Fe systems above, ΔG shifts by more than 1 kcal mol^{-1} between 5 and 45 °C and K_{eq} shifts by almost an order of magnitude. This effect does not appear to have been incorporated into most applications of modern PCET theories to either small molecule or enzymatic systems.¹⁹ In particular, variation in ΔG indicates changes in the shape of the free energy surface which should affect processes involving hydrogen tunneling. Does the variation in ΔG play a role, for instance, in the unusual temperature dependence of the kinetic isotope effect for HAT from a fatty acid to the nonheme iron center in lipoyxygenase enzymes? Since large values of $|\Delta S_{\text{ET}}^{\circ}|$ have been observed in biological systems,^{75,76} the close connection between $\Delta S_{\text{ET}}^{\circ}$ and $\Delta S_{\text{HAT}}^{\circ}$ described here suggests that there are significant entropic contributions in HAT and PCET reactions of metalloproteins.

4. Conclusions

Ground state entropy changes for hydrogen atom transfer reactions, $\Delta S_{\text{HAT}}^{\circ}$, vary substantially depending on the reaction. Values reported vary from $-41 \pm 2 \text{ cal mol}^{-1} \text{ K}^{-1}$ for HAT from a cobalt(II) 2,2'-bi-2-imidazole complex to the nitroxyl radical TEMPO (eq 3), to $-2 \pm 3 \text{ cal mol}^{-1} \text{ K}^{-1}$ for HAT from TEMPOH to the stable aryloxy radical 'Bu₃PhO' (eq 8). These values have been determined by van't Hoff analysis of equilibrium data, by calorimetric measurements, and using thermochemical cycles. These data and those from previous reports show that the magnitude of $|\Delta S_{\text{HAT}}^{\circ}|$ for reactions with TEMPO have the following trend: **Co^{II}(H₂bim) > Fe^{II}(H₂bip) = Fe^{II}(H₂bim) > Ru^{II}(py-imH) \approx 'Bu₃PhOH \approx 0.** The analysis presented here supports the long-standing assumptions that $\Delta S_{\text{HAT}}^{\circ} \approx 0$ and that $S^{\circ}[\text{AH}] \approx S^{\circ}[\text{A}]$ for HAT reactions of organic and small gas phase molecules, but not for transition metal complexes. Analyses of transition metal HAT reactions need to take into account the frequently large reaction entropies and should not be based just on bond dissociation enthalpies. The trend in $\Delta S_{\text{HAT}}^{\circ}$ for the metal complexes is the same as that observed for electron transfer half-reaction entropies in aprotic solvents $\Delta S_{\text{ET}}^{\circ}$, and the magnitudes of these values are often similar as well. This analogy is a result of both the HAT and ET values being significantly influenced by vibrational entropy contributions. The more extensive database of electron transfer entropies therefore provides guidelines for initial predictions of hydrogen transfer entropies.

- (70) Similar differences in $\Delta S_{\text{ET}}^{\circ}$ are seen for hexaaquo (22 $\text{cal mol}^{-1} \text{ K}^{-1}$),^{62,72} tris-ethylenediamine ($20 \pm 4 \text{ cal mol}^{-1} \text{ K}^{-1}$),^{60a} and tris-2,2'-bipyridine ($19 \pm 3 \text{ cal mol}^{-1} \text{ K}^{-1}$)⁵⁹ complexes of Co and Ru.
- (71) On the other hand, the value of the ET entropy for a single complex is highly solvent dependent. $\Delta S_{\text{ET}}^{\circ}$ for $[\text{Ru}(\text{tacn})_3]^{3+/2+}$, for example, is 26.2, 31.1, and 8.6 $\text{cal mol}^{-1} \text{ K}^{-1}$ in DMSO, acetone, and water, respectively (tacn = 1,4,7-triazacyclononane).^{60a} For aqueous $[\text{M}(\text{OH}_2)_6]^{3+/2+}$ ions and related species, the strong hydrogen bonding can lead to large solvent contributions to $\Delta S_{\text{ET}}^{\circ}$.⁶⁷
- (72) Yee, E. L.; Cave, R. J.; Guyer, K. L.; Tyma, P. D.; Weaver, M. J. *J. Am. Chem. Soc.* **1979**, *101*, 1131–1137.
- (73) $\Delta S_{\text{ET}}^{\circ}$ for Co^{III}/Co^{II} redox couples in protic media vary more widely (-6 to $+60 \text{ cal mol}^{-1} \text{ K}^{-1}$)⁶² because other effects can contribute.⁶⁷
- (74) For example, $[\text{Fe}(\text{phen})_3]^{3+/2+}$ (phen = phenanthroline) is low-spin for both Fe^{III} and Fe^{II} and has $\Delta S_{\text{ET}}^{\circ} = 25.4 \pm 2 \text{ cal mol}^{-1} \text{ K}^{-1}$ in MeCN, similar to $[\text{Ru}(\text{bpy})_3]^{3+/2+}$ (27 $\text{cal mol}^{-1} \text{ K}^{-1}$).^{59dg} $[\text{Fe}(\text{tacn})_2]^{3+/2+}$ has $\Delta S_{\text{ET}}^{\circ} = 36.3 \text{ cal mol}^{-1} \text{ K}^{-1}$ in MeCN; 29.2 $\text{cal mol}^{-1} \text{ K}^{-1}$ when the spin-equilibrium contribution at Fe^{II} is removed.^{60a} $[\text{Ru}(\text{tacn})_2]^{3+/2+} = 27.9 \text{ cal mol}^{-1} \text{ K}^{-1}$ in MeCN.^{60a}

- (75) (a) Farhangrazi, Z. S.; Fosett, M. E.; Powers, L. S.; Ellis, W. R. Jr. *Biochemistry* **1995**, *34*, 2866–2871. (b) Sailasuta, N.; Anson, F. C.; Gray, H. B. *J. Am. Chem. Soc.* **1979**, *101*, 455–458. (c) Ellis, W. R., Jr.; Wang, H.; Blair, D. F.; Gray, H. B.; Chan, S. I. *Biochemistry* **1986**, *25*, 161–167.
- (76) (a) Taniguchi, V. T.; Sailasuta-Scott, N.; Anson, F. C.; Gray, H. B. *Pure Appl. Chem.* **1980**, *52*, 2275–2281. (b) Battistuzzi, G.; Borsari, M.; Sola, M. *Eur. J. Inorg. Chem.* **2001**, *2001*, 2989–3004.

5. Experimental Section

5.1. General Considerations. All manipulations were carried out under anaerobic conditions in MeCN using standard high-vacuum line and nitrogen-filled glovebox techniques unless otherwise noted. NMR spectra were acquired on Bruker Avance-500, DRX-499, Avance-300, or Avance-301 spectrometers. Static UV–visible spectra were obtained using either a Hewlett-Packard 5483 spectrophotometer equipped with an eight-cell holder thermostated with a Thermo-Neslab RTE-740 waterbath or a Shimadzu UV-2401 PC dual beam instrument. Spectra are reported as λ_{max} , nm [ϵ , $\text{M}^{-1} \text{cm}^{-1}$] and were blanked relative to pure MeCN. Air-sensitive samples were prepared in the glovebox, and their spectra were taken using either quartz cuvettes attached to Teflon-stoppered valves (Kontes) or injectable screw-capped cuvettes with silicone/PFTE septa (Spectrocell). Septa were replaced after each experiment. Rapid kinetic measurements were taken using an OLIS USA stopped-flow instrument equipped with the OLIS-rapid scanning monochromator and UV–vis detector and thermostated by a Neslab RTE-111 waterbath. All errors are reported as $\pm 2\sigma$ based on fits weighted with the errors propagated from experimental measurements.

5.2. Materials. Low water content CH_3CN (<10 ppm H_2O ; Allied Signal/Burdick and Jackson brand) was taken from a steel keg sparged with Ar and dispensed through the glovebox. CD_3CN (Cambridge Isotopes Laboratories) was dried by stirring overnight with CaH_2 , vacuum transferring, and stirring briefly (<1 h) over P_2O_5 , vacuum transferring back over CaH_2 for ca. 30 min, and then storing in the glovebox free of drying agent. Other solvents were dried using a “Grubbs-type” Seca Solvent System installed by GlassContour.⁷⁷ 2,2,6,6-Tetramethyl-1-piperidinyloxy (TEMPO; Acros Organic and Aldrich) was sublimed at room temperature under static vacuum before use. $[\text{Fe}^{\text{II}}(\text{H}_2\text{bip})_3][\text{ClO}_4]_2$, $(\text{Fe}^{\text{II}}(\text{H}_2\text{bip}))$,³¹ $[\text{Fe}^{\text{III}}(\text{H}_2\text{bip})_2(\text{Hbip})][\text{ClO}_4]_2$ ($\text{Fe}^{\text{III}}(\text{Hbip}))$,³¹ $[\text{Co}^{\text{II}}(\text{H}_2\text{bim})_3][\text{ClO}_4]_2$, $(\text{Co}^{\text{II}}(\text{H}_2\text{bim}))$,³¹ $[\text{Co}^{\text{III}}(\text{Hbim})(\text{H}_2\text{bim})_2][\text{ClO}_4]_2$ ($\text{Co}^{\text{III}}(\text{Hbim}))$,³¹ $[\text{Ru}^{\text{II}}(\text{acac})_2(\text{py-imH})]$, $(\text{Ru}^{\text{II}}(\text{py-imH}))$,³² $[\text{Ru}^{\text{III}}(\text{acac})_2(\text{py-im})]$, $(\text{Ru}^{\text{III}}(\text{py-im}))$,³² 2,2,6,6-tetramethyl-1-piperidinyloxy (TEMPOH),^{28,78} and 2,4,6-tri-*tert*-butyl phenoxyl ($^t\text{Bu}_3\text{PhO}^\bullet$)³³ were prepared and characterized following literature procedures. All other reagents were purchased from Aldrich and used as received. *Caution: The perchlorate salts used herein are potentially explosive and should be handled with care in small quantities only. They should not be heated when dry or subjected to friction or shock, such as scratching with a non-Teflon-coated spatula.*

5.3. Solution K_{eq} Measurements. Equilibrium experiments for $\text{Fe}^{\text{II}}(\text{H}_2\text{bip})$ and $\text{Fe}^{\text{II}}(\text{H}_2\text{bim}) + \text{TEMPO}$ have been previously reported.²⁸ K_3 values for $\text{Co}^{\text{II}}(\text{H}_2\text{bim}) + \text{TEMPO} \rightleftharpoons \text{Co}^{\text{III}}(\text{Hbim}) + \text{TEMPOH}$ were directly measured by ^1H NMR spectroscopy. A set of J-Young capped NMR tubes were charged with varying amounts of TEMPO (5–10 mg, 0.03–0.06 mmol), leaving one tube empty to act as a “time zero” spectrum. To each of these tubes was added a 0.4 mL aliquot of a stock solution of $\text{Co}^{\text{II}}(\text{H}_2\text{bim})$ (11 mM in CD_3CN containing 3–10 μL CH_2Cl_2 as an integration standard). After mixing, the tubes were quickly removed from the glovebox and placed in a thermal bath. Changes in the NMR spectrum were monitored over the course of 2–7 days depending on the temperature. Data acquisition was stopped when the integrations for each species remained constant for a minimum of 12 h. The tubes were then placed at room temperature (21 °C) and allowed to re-equilibrate for 2–7 days, again monitored by ^1H NMR spectroscopy. Reliable integrations were obtained using Mestre-C by manually phasing and baselining the spectrum from +60 to –3 ppm, as well as adjusting the phase and bias for each integral. Integrations were found to be reproducible to ± 3 –5% based on the standard deviation of three spectra taken in rapid succession

Table 3. Standard Conditions and Integration Times for Calorimetry Reactions

reaction	inner chamber	outer chamber	integration time
$\text{Fe}^{\text{II}}(\text{H}_2\text{bip}) + \text{TEMPO}^a$	2.8 mM	23–109 mM	$\sim 10\,000$ s
$\text{Ru}^{\text{II}}(\text{py-imH}) + ^t\text{Bu}_3\text{PhO}^\bullet$	$\text{Fe}^{\text{II}}(\text{H}_2\text{bip})$ 5–10 mM	TEMPO ^a 11 mM	~ 2000 s
$\text{Ru}^{\text{II}}(\text{py-imH}) + \text{TEMPO}$	$\text{Ru}^{\text{II}}(\text{py-imH})$ 10 mM	$^t\text{Bu}_3\text{PhO}^\bullet$ 11 mM	~ 4000 s
$\text{Co}^{\text{II}}(\text{H}_2\text{bim}) + ^t\text{Bu}_3\text{PhO}^\bullet$	$\text{Ru}^{\text{II}}(\text{py-imH})$ 6.2 mM	TEMPO 4.4 mM	~ 8000 s
$\text{TEMPOH} + ^t\text{Bu}_3\text{PhO}^\bullet$	$\text{Co}^{\text{II}}(\text{H}_2\text{bim})$ 11 mM	$^t\text{Bu}_3\text{PhO}^\bullet$ 14.7 mM	~ 4000 s
	TEMPOH	$^t\text{Bu}_3\text{PhO}^\bullet$	

^a At 29.6 °C, $\text{Fe}^{\text{II}}(\text{H}_2\text{bip}) + \text{TEMPO}$ has $K_{\text{eq}} = 1.7 \pm 0.3$. To ensure that the reaction went to completion, 8–34 equiv of TEMPO were used.

on a tube at equilibrium. K_4 values were obtained from the ratio of the following integration regions: $\text{Co}^{\text{II}}(\text{H}_2\text{bim})$ 24.7–21.2 ppm, $\text{Co}^{\text{III}}(\text{Hbim})$ 4.85–2.68 ppm, TEMPO 21.2–10.8 ppm, TEMPOH 1.73–1.34 ppm, from at least two spectra.

The equilibrium constant for $[\text{Ru}^{\text{II}}(\text{hfac})_2(\text{py-imH})] + ^t\text{Bu}_3\text{PhO}^\bullet \rightleftharpoons [\text{Ru}^{\text{II}}(\text{hfac})_2(\text{py-im})] + ^t\text{Bu}_3\text{PhOH}$ (eq 7) was measured by UV–vis titration using the method used in ref 32 to determine K_7 , using a solution of $\text{Ru}^{\text{II}}(\text{hfac})_2(\text{py-imH})$ (0.027 mM, 2.5 mL) titrating with $^t\text{Bu}_3\text{PhO}^\bullet$ (6.7 mM) until 10 equiv (10 μL = 1 equiv). The UV–vis data were analyzed using the absorbance at 481 nm to determine equilibrium constant $K_7 = 0.062 \pm 0.013$ ($\Delta G^\circ_7 = 1.6 \pm 0.1 \text{ kcal mol}^{-1}$) from the average of two runs. Since $\Delta G^\circ_7 = \text{BDFE}[\text{Ru}^{\text{II}}(\text{hfac})_2(\text{py-imH})]_{\text{MeCN}} - \text{BDFE}(^t\text{Bu}_3\text{PhOH})_{\text{MeCN}}$ and $\text{BDFE}[\text{Ru}^{\text{II}}(\text{hfac})_2(\text{py-imH})] = 79.6 \pm 1.0$ (from E° and $\text{p}K_a$ values³²), this yields $\text{BDFE}(^t\text{Bu}_3\text{PhOH})_{\text{MeCN}} = 78 \pm 1$.

5.4. Calorimetry. Experiments were done on a Setaram C-80 Calvet calorimeter outfitted with a pair of Hastelloy C276 Reversal Mixing cells (utilizing the larger 2.5 mL reaction cup and graphited Teflon seals) under isothermal conditions. In the calorimeter, each cell is surrounded by an electrical heater coil. The difference in current required to maintain a constant temperature between the two cells is related to the heat evolved from the reaction. The methodology used is a modification of literature procedures.^{34,35} The calorimeter was set at 30.0 °C and had an actual sample temperature of 29.6 ± 0.1 °C. The calorimeter had been previously calibrated with a Joule-effect vessel, and the calibration was checked intermittently using the standardized aqueous heat of solution for KCl.

In a glovebox, the inner cup of one cell was charged with 5–15 mg of limiting reagent in 2.0 mL of MeCN and covered with a Hastelloy cap. The outer chamber was charged with 1.0 mL of the reagent in slight excess (1.1–2.0 equiv), and the remainder of the cell was assembled. See Table 3 for typical concentrations. The reference cell was assembled under identical conditions using a total of 3.0 mL of MeCN. The sealed cells were removed from the glovebox and thermally equilibrated in the calorimeter until both the flux and the temperature had reached steady state (ca. 1–2 h). This was deemed the experimental baseline, and the reaction was initiated by rotation of the calorimeter body, which inverted the cells and allowed the two solutions to mix. The heat flux was then recorded until the baseline was once again achieved. The resulting fluxogram was integrated using SetSoft-2000 to give the heat evolved (Table 3). After the reaction was complete, the sample cell was removed from the calorimeter and returned to the glovebox. The final reaction mixture was diluted in a Kontes-valve cuvette (0.1 mL of sample in ca. 2.0 mL of MeCN) and an optical spectrum was obtained, to determine that the reaction had gone to completion and remained uncontaminated by air. Reactions were repeated a minimum of three times to achieve the desired level of reproducibility. Control reactions for the heats of dilution were measured for each reagent under similar concentration regimes to the actual reaction conditions. In most cases these were found to be small effects.

(77) Pangborn, A. B.; Giardello, M. A.; Grubbs, R. H.; Rosen, R. K.; Timmers, F. J *Organometallics* **1996**, *15*, 1518–1520, See also <http://www.glasscontour.com/index.html>.

(78) Ozinskas, A. J.; Bobst, A. M. *Helv. Chim. Acta* **1980**, *63*, 1407–1411.

5.5. Calculations. All calculations were performed using Gaussian03.⁷⁹ *t*Bu₃PhOH and [•]Bu₃PhO were optimized in C₁ symmetry, and geometries were confirmed to be local minima by vibrational analysis. Following literature precedent,⁵¹ the B3LYP functional was used with the 6-31+G basis set with additional (*p*) polarization functions on hydrogen atoms only. Radical species were computed using the restricted-open shell (RO) formalism. Bakalbassis et al. found this (RO)B3LYP/6-31+G(*p*) method (the nonstandard basis set nomenclature indicates that polarization functions are included for hydrogen atoms only and not heavy atoms) produced chemically accurate values of BDE for several phenolic compounds.⁵¹ Solution enthalpies and free energies were obtained from geometry optimizations and frequency analyses including a polarizable continuum model (PCM)⁸⁰ of acetonitrile, as implemented in Gaussian03.⁸¹ Free energies of solution, $\Delta G_{\text{soln}}^\ddagger$, were also obtained from PCM single-point calculations on the gas phase optimized geometries, with the inclusion of the SCFVAC keyword; for these calculations atomic radii from the United Atom Topological

Model (UAHF) were used. The values of $\Delta G_{\text{soln}}^\ddagger[\text{[•]Bu}_3\text{PhO}]_{\text{MeCN}} - \Delta G_{\text{soln}}^\ddagger[\text{[•]Bu}_3\text{PhOH}]_{\text{MeCN}}$ computed via these two methods are essentially identical (within ca. 0.01 kcal mol⁻¹).

Acknowledgment. We gratefully acknowledge financial support from the U.S. National Institutes of Health (Grant GM50422), the National Research Council of Canada (NSERC) (for a fellowship to E.A.M.), the UW Department of Chemistry, and the Office of Science, Office of Basic Energy Sciences under Contract DE-AC06 RLO 1830. We thank Drs. T. S. Autrey, D. M. Camaioni, and A. J. Karkamkar for assistance with the calorimetry experiments; C. Isborn and Dr. X. Li for assistance with PCM calculations; and J. J. Warren for his thoughtful comments.

Supporting Information Available: Detailed calorimetric traces, integrations, reaction spectra, complete ref 79, and calculated data are provided. This material is available free of charge via the Internet at <http://pubs.acs.org>.

(79) Frisch, M. J.; et al. *Gaussian 03*, revision D.02, 2004. See Supporting Information for full citation.

(80) (a) Cancès, M. T.; Mennucci, B.; Tomasi, J. *J. Chem. Phys.* **1997**, *107*, 3032–3041. (b) Cossi, M.; Barone, V.; Mennucci, B.; Tomasi, J. *Chem. Phys. Lett.* **1998**, *286*, 253–260. (c) Mennucci, B.; Tomasi, J. *J. Chem. Phys.* **1997**, *106*, 5151–5158.

JA8081846

(81) Cossi, M.; Scalmani, G.; Rega, N.; Barone, V. *J. Chem. Phys.* **2002**, *117*, 43–54.